MODELING AND VALIDATION OF CROP FEEDING IN A LARGE SQUARE BALER

A Thesis Submitted to the

College of Graduate Studies and Research

in Partial Fulfillment of the Requirements

for the Degree of Master of Science in the

Department of Agricultural and Bioresource Engineering

University of Saskatchewan

Saskatoon,

Saskatchewan

By

Tyler Remoué

PERMISSION TO USE

In presenting this thesis in partial fulfillment of the requirements for a degree of Master of Science from the University of Saskatchewan, I agree that the libraries of this University may make it freely available for inspection. I further agree that permission for copying this thesis in any manner, in whole or in part for scholarly purposes may be granted by the professor who supervised my thesis work or, in his absence, by the Head of the Department or the Dean of the College in which my thesis work was done. Copying or publication or use of this thesis or parts thereof for financial gain without the author's written permission is prohibited. It is understood that due recognition shall be given to the author and to the University of Saskatchewan for any scholarly use of material contained in this thesis.

Requests for permission to copy or to make other use of material in this thesis in whole or in part should be addressed to:

Head of the Department of Agricultural and Bioresource Engineering:

University of Saskatchewan

57 Campus Drive

Saskatoon, SK. Canada

S7N 5A9

ABSTRACT

This study investigated the crop density in a New Holland BB960 (branch of CNH Global N.V.) large square baler as examined by crop trajectory from the precompression room to the bale chamber. This study also examined both the top and bottom plunger pressures and critical factors affecting the final top and bottom bale densities.

The crop trajectories (wad of crop) were measured using a high-speed camera from the side of the baler through viewing windows. The viewing windows were divided into four regions for determining the crop displacement, velocity and acceleration. Crop strain was used to evaluate the potential change in density of the crop before being compressed by the plunger. Generally, the vertical crop strain was found to be higher in the top half of the bale compared to the bottom. Average strain values for side measurements were 12.8% for the top and 2.1% for the bottom.

Plunger pressures were measured to compare peak pressures between the top and bottom halves of each compressed wad of crop, and to develop pressure profiles based on the plunger's position. Results of comparing the mean peak plunger pressures between the top and bottom locations indicated the mean pressures were significantly higher at the top location with the exception of one particular setting. Resulting pressure profile graphs aided in qualitatively describing the compression process for both top and bottom locations.

A stepwise regression model was developed to examine the difference in material quantity in the top half of the bale compared to the bottom, based on bale weights. The model indicated that flake setting, stuffer ratio and number of flakes had the greatest effect on maintaining consistent bale density by comparing top to bottom halves of each bale. The R^2 (coefficient of determination) value for the developed model was of 59.9%. The R^2 was low although could be accounted for due to the limited number of data points in the developed model.

ACKNOWLEDGEMENTS

I wish to acknowledge the numerous people who have provided support, technical assistance and guidance over the course of this study. Without their contributions, this study would not have been possible.

- The financial support of CNH Europe N.V., CNH America LLC and the NSERC CRD program is greatly acknowledged for making this project possible.
- My advisor, Dr. Martin Roberge, for his unparalleled support, providing a wealth of opportunity and encouragement as well as being a mentor.
- Advisory committee members, Dr. Trever Crowe and Dr. Huiqing Guo, for overseeing the research and providing valuable insight.
- Special thanks to my industrial supervisor Mr. Ad Naaktgeboren and the CNH Large Square Baler team. Their friendly expertise and wisdom have created a rewarding experience and they were fun to work with. I would especially like to extend my thanks to Mr. Stefan Derycke, Mr. Olivier Vanhercke, Mr. Karel Naeyaert, Mr. Werner Vlaeminck and others for their support.
- Mr. John Posselius, Mr. Kevin Smith, Mr. Tim Douglas and the CNH America team for their knowledge and assistance over the course of this research.
- Mr. Bob Benneweis for his assistance with CAN software and hardware.
- Mr. Mike Miller, Mr. Louis Roth, Mr. Wayne Morley and the rest of the Agricultural and Bioresource Engineering staff.
- Mr. James Schnaider for his assistance during almost every stage of the research and for being a lot of fun to work with.

DEDICATION

I wish to dedicate this to my parents for always being there to support me and providing me with so much opportunity in life. My only hope is that I will be as strong, patient, hard working and caring with my own children as my parents were with me.

TABLE OF CONTENTS

LIST OF TABLES

LIST OF FIGURES

LIST OF ABBREVIATIONS

%DiffWT	percent difference in weight
A	experimental factor
$a_{vertical}$	vertical acceleration (m/s^2)
B	experimental factor
C	experimental factor
C	experimental factor
CAD	computer aided design
CAN	controller area network
CCD	charge-coupled device
ChamPress	bale chamber hydraulic pressure (MPa)
CPU	central processing unit
D	compression chamber depth (m)
Δ	crop strain
DiffPress	difference in pressure between top and bottom plunger sensors (kPa)
DiffWT	difference between F_{Top} and F_{Bottom} (kg)
DMFR	dry mass flow rate (kg/s)
DVC	digital video camera
Eh	modulus of elasticity (kPa)
F	Force applied by plunger (N)
F_{Bottom}	measured mass from bottom half of bale (kg)
Fh	coefficient of friction between crop and bale chamber
FlakeSet	setting for flake thickness (out of 10)
F_{Top}	measured mass from top half of bale (kg)
HSC	high speed camera
IR	Infrared
ISO	international standardization organization
K	material coefficient
Kg	kilograms
L	length of converging section (m)
LED	light emitting diode
M	meters
m_e	experimental factor
Mm	millimeters
N	experimental factor
NumFlake	total number of flakes in the bale
P	Specific pressure acting on plunger (Pa)
PIV	particle image velocimetry
PLoad	percent load (%)
PTO	power take off
S	samples
S	seconds
StuffR	stuffer ratio
T	thickness of plate (in)
T	time (ms)

V	velocity of compression (m/s)
VBA	visual basic application
VFR	volumetric flow rate (m^3/s)
$v_{vertical}$	vertical velocity (m/s)
W	moisture content dry basis (%)
W	width of compression chamber (m)
WT	mass (kg)
$WT\ Total$	total mass of the bale (kg)
y_c	total convergence (mm)
Y	dependent variable
y_v	vertical position (mm)
A	significance level
B	experimental factor (m/s)
P	density of compressed hay (kg/m^3)
Po	density of hay before being compressed (kg/m^3)
σ	Maximum tensile stress of plate (lbs/in^2)

1. INTRODUCTION

Hay is an important aspect of Canada's agricultural economy. Six million hectares are devoted annually for the production of cultivated tame hay and fodder crops. The produced hay is commonly used either domestically, to maintain livestock during the winter, or used to supply one of Canada's two primary forage processing industries; alfalfa dehydration or hay compaction. Both industries are highly export oriented and contribute to maintaining Canada's vibrant and diverse forage sector. To date, Canada is the world's largest exporter of alfalfa pellets and the second largest exporter of alfalfa cubes. The industry produces 350,000 tonnes of alfalfa pellets and 225,000 tonnes of alfalfa cubes annually. The Canadian double compressed bale industry has encountered dramatic growth within the last four years and the current total production is approximately 260,000 tonnes of hay annually (Agriculture and Agri-Food Canada 2006).

The exchange of hay between buyer and seller is largely dependent on quality. Whether the hay is marketed from farmer to farmer or on a global scale, quality has a large impact on the success of the sale. To facilitate marketing, producers have generally relied on a system of describing the product based on physical and nutritional attributes. Accurate measurement of these market-driving features depends on how consistent the product is dispersed throughout the package, or packages, being sold.

In the last 15 years, large square balers have become popular among hay producers. Large square bales have been an attractive alternative compared to large round bales due to the ease of handling and stacking for transportation purposes which is especially beneficial in marketing hay off the farm (National Agrability Project 2003). The disadvantage of large square bales is the high initial equipment cost and hence, most owners are either large scale hay producers or custom operators. These producers/operators generally demand quality machines to meet the needs of buyers or cliental.

Manufacturers of large square balers concentrate on designing machines which maximize the density of the formed material and ensure the density is consistent throughout each bale. Maximizing the density of the formed bales reduces storage, transportation and handling costs provided the input energy to produce the package is at a cost-effective level (Neale 1986). Constant-density bales ensure the bales are of uniform weight and suggest uniform distribution of nutrients and moisture.

For a feed manufacturer, maintaining uniform material distribution can be a significant factor due to legal obligations. In Canada, the legal requirements for labelling feeds are enforced by the federal Feeds Act, administered by the Canadian Food Inspection Agency (Canadian Food Inspection Agency 2005). In the US, the legal requirements for labelling feeds are enforced by the Uniform State Feed Bill, administered by the Association of the American Feed Control Officials (Perry et al. 1999). Accurate labelling and mixing of hay products could become problematic if the purchased hay is not a consistent product.

Uniform, high-density bales are key factors of quality hay. Uniform filling of the bale chamber produces bales with sharp, crisp corners which are characteristics of superior bales. Large variations in bale density can cause the bale to lose its form and possibly take the shape informally known as a "Banana Bale". Hay producers view these bales as substandard. Producers recognize the value in accurately defining their product to increase its marketability.

The purpose of the precompression room is to provide a stage to pre-compact the crop prior to being compressed by the plunger and provide the means to convey the crop in front of the plunger. The goal of this study was to analyze the flow pattern of the crop leaving the precompression room before reaching its final vertical position and being further compressed by the plunger. Depending on how the crop is situated before being compressed, the consistency of the crop dispersion throughout each bale will vary.

The bale chamber walls could affect the density of the crop as the walls apply pressure to mould the bale into its final shape. Converging bends manufactured into the bale chamber walls create a funnel effect, causing the crop to be squeezed as the bale is pushed through the bale chamber.

The effects of the bale chamber walls on maintaining uniform density may have a significant impact on the formation of a consistent product.

This thesis is organized by analyzing two distinct experiments; measuring the flow pattern of crop leaving the precompression room and compression of the crop by the plunger. The literature review in Section 2 outlines measurement of crop flow and crop compaction and as an extension, discusses the operation and evolution of large square balers. The objectives for this research are presented in Section 3, followed by the procedures and analysis used to fulfill these objectives in Sections 4 and 5. Sections 6 and 7 discuss the results and conclusions from the experiments followed by Section 8, which outlines future recommendations.

2. LITERATURE REVIEW/BACKGROUND

2.1. Brief History of the Large Square Baler

Baling hay is a process of reducing the material volume to achieve a defined package (generally round or square) which facilitates handling and preserves material quality for future use (Sitkei 1986). Mechanical means for baling hay were established in the late 19th century with the development of the stationary hay baler, and advancements in the early 1900's lead to the first mobile balers. The first mobile balers produced rectangular bales approximately 350 x 450 x 1000 mm in dimension and operated on the principle of lifting the crop, compressing the crop and tying retaining strings when bales reached a desired length.

Major developments in baler technology occurred during the early 1970's with the availability of the first large balers, specifically the Howard baler followed by the first of the round balers. The Howard baler (manufactured by the Howard Rotovator Company Ltd.) was a large square baler producing low density bales (approximately 65 kg/m^3) with approximate bale dimensions of 1.5x1.5x2.4 m. A key advancement in the large square baler industry occurred during the late 1970's with the introduction of the Hesston 4800 (Hesston, KS). This baler operated on the same principles as the previous square balers although incorporated a precompression room that compacted the crop before it was swept in front of the plunger. The precompression room greatly increased the bale densities to produce bales with densities up to 160 kg/m^3. The inclusion of precompression rooms was soon incorporated by other manufactures of large square balers.

Other noteworthy machines used to produce high-density bales were the Welger Delta 5000, Vicon HP 1600 and Agricultural & Foods Research Council (AFRC) experimental baler. The Welger Delta 5000 produced flat wafers 0.4 x 1.2 x 1.5-2.5 m and used an accumulator so that three wafers could be stacked together. The densities of the wafers were approximately 130 kg/m^3. The Vicon HP 1600 produced bales using a hydraulic ram to compress 5 to 8 flakes of crop against a closed-ended chamber before being tied and ejected from the baler. The Vicon

baler produced bales of approximately 170 kg/m^3 in density and used wire ties instead of twine, which meant either fewer ties were needed or more material could be held with the same compacting force. Another baler producing bales of approximately 200 kg/m^3 was developed by AFRC Engineering in Silsoe, UK. The baler operated by compressing the crop in a closed-ended column chamber. Once the pressure in the chamber reached a threshold sensed by the tailgate, cleavers were introduced to separate the formed bale and press the crop against the closed tailgate. The bale was then tied and the tailgate opened to eject the bale. This baler was never realized commercially although it produced bales 30% greater in density than the bales produced by the Delta or Hesston balers (Neale 1986; Neale 1989; Stewart 1985).

2.2. Baler Operation

Knowledge of the baler operation is fundamental to understand the mechanics of this study. This section briefly describes the operation of the large square baler used in this research and outlines important aspects for future reference.

The machine used for research was a New Holland BB960 large square baler as illustrated in Figure 2.1. The baler operates on a two stage feeding system (Figure 2.2). Crop is lifted from windrows into the baler by the pickup (1). The pickup pushes the crop into the precompression room (2) by means of packing fingers (3). The packing fingers intertwine the crop together and pack the precompression room. The precompression room functions as the first stage for crop compression. Crop is prevented from moving into the bale chamber by holding fingers at the top of the precompression room. Once the pressure in the precompression room reaches a predetermined value, the stuffer sensing mechanism causes the holding fingers to release and the stuffer forks (4) to activate. The stuffer forks thrust the wad of crop directly in front of the plunger (5) where it is compressed into a flake. The stuffer forks and holding fingers return to their original stationary state after the crop has been released from the precompression room. For the purposes of this study, a distinct element of crop before the crop has been compressed by the plunger will be termed a wad of crop and after compression will be termed a flake.

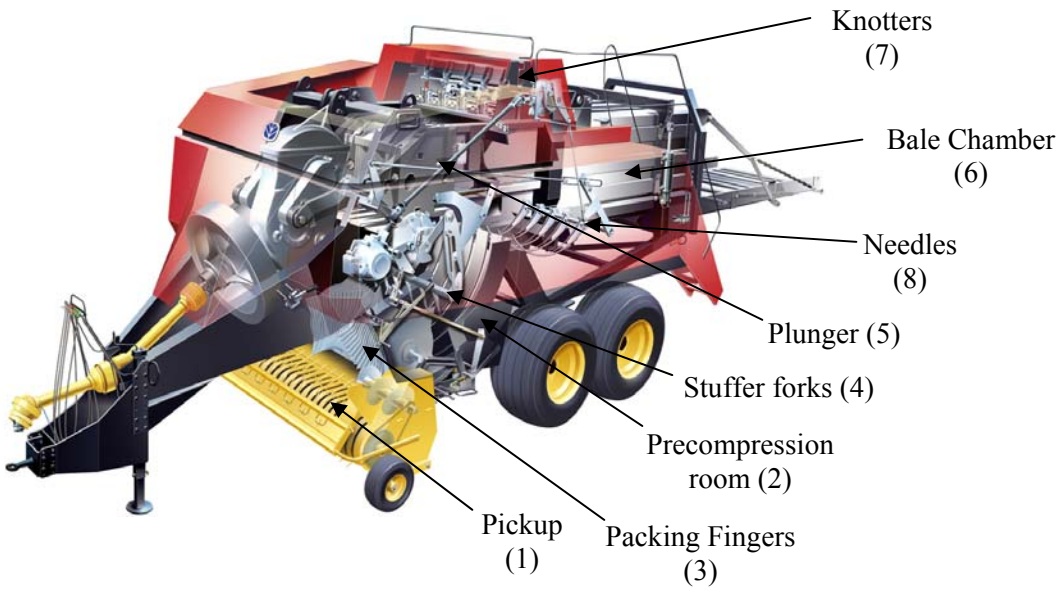

Figure 2.1 Cutaway view of BB960 (Courtesy of CNH Europe).

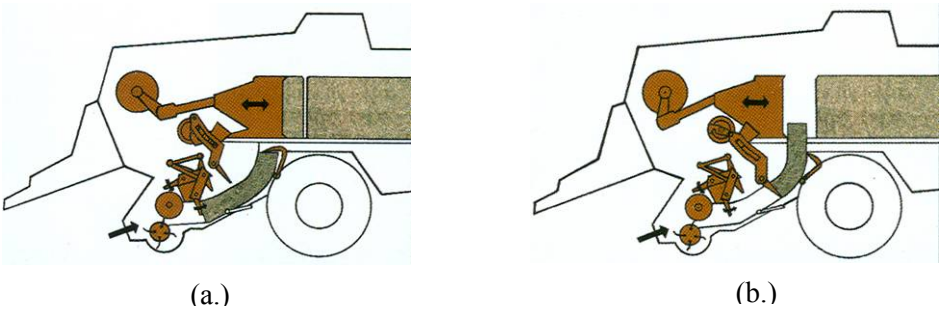

Figure 2.2 (a) Packing the precompression room and (b) crop entering bale chamber (Courtesy of CNH Europe).

Figure 2.3 illustrates a side view into the compression chamber of a large square baler. The figure shown illustrates a large square baler with holes cut through the side walls into the compression chamber. Crop is ejected from the bottom of the windows to directly in front of the plunger where it is compressed into a flake.

Figure 2.3 View into the side of the compression chamber of a large square baler. Crop will enter from the bottom of the windows then be compressed by the plunger into a flake.

2.2.1. Density Control

As the bale chamber walls may have an effect on variations in density, this section outlines the different modes of operating the bale chamber walls. These modes were used to configure the baler during field experiments and the settings were included as factors in a mathematical model to investigate density indifferences.

After the wad is injected into the bale chamber (6), it is compressed by the plunger against previously formed flakes. Pressure exerted by the walls of the bale chamber dictates the frictional force required to overcome static friction and shift the flakes in the chamber. An increased force to shift the flakes causes the plunger to compact the flakes tighter, producing a higher density bale. Hence, the bale compression room walls are the foremost mechanism to control the density of the bales produced.

The bale chamber has three moving walls (top and sides) controlled by two hydraulically controlled linear actuators connected to a cam mechanism. To operate the linear actuators, the baler uses its own on-board hydraulic circuit, separate from the tractor's hydraulics. The complete on-board hydraulic circuit forms the bale density system and can be controlled in three

different ways; automatic bale density control, manual bale density control and manual override bale density control.

The automatic bale density control is the most typical setting used to control the bale density. In this mode, the baler uses feedback from an electronic load sensor to adjust the hydraulic pressure controlling the linear actuators connected to the bale chamber walls. The load sensor was mounted in the plunger to measure the force of each plunger stroke, and at the time of the tests, was factory-installed equipment. The chamber wall orientations, hence hydraulic/wall pressures, were adjusted so that each applied plunger force was consistent, producing bales of uniform density set by the operator. Bale density was based on a relative scale from 0 to 100, with 0 relating to the lowest relative load and 100 relating to the maximum load limit based on the design of the machine.

The manual bale density control is used when the load sensor fails to function while all other sensors are still operational. The operator manually selects the hydraulic pressure acting on the linear actuators controlling the bale chamber walls. Constant pressure is maintained and is set through the electronic control system.

The manual override bale density control is used when the electronic control system malfunctions. A manual valve located on the side of the machine is used to set the hydraulic pressure of the linear actuators. The pressure is set by operating the baler and turning an adjusting screw to a selected value displayed by a mechanical pressure gage on the front of the baler.

2.2.2. Bale Tying

Bale tying signifies the completion of a formed bale and indicates the beginning of a new bale. For research purposes, the knotter cycle provides an excellent reference to obtain the start and stop sequences when collecting data. Understanding the mechanism of the knotter operation is important to identifying the bounds of particular data sets.

As the bale being formed was pushed rearward by the plunger, the movement of the bale turned a length-metering wheel. The rotation of the metering wheel determined the bale length based

on effective circumference of the wheel. Once the metering wheel measured a set bale length, the knotters (7 see Figure 2.1) are activated to tie the twines around the formed bale. The knotter cycle is synchronized with the plunger position and occurs when the plunger is near its most rearward position.

There were two balls of twine associated with each knotter. One ball supplied the knotter located above the compression chamber and the other supplied the needles (8 see Figure 2.1) located below the compression chamber. During knotter operation, the needles bring the twine from below up towards the knotters. Before the needles reach the knotter, the needles also pick up the upper set of twines. Both twines are tied together in the knotters, and the ends are cut to complete the bale. On the needles' return stroke, the remaining twine ends are held and a second knot is tied. The needles then retract to their original state, forming the start of the next bale (New Holland BB960 Operator's Manual 1999).

2.3. Particle Tracking

Examining particle movement from the precompression room to the bale chamber is an important aspect to identify the flow pattern of crop during its trajectory. Understanding the kinematics of particle movement during this stage aids in addressing potential issues with density variations. In order to quantify the characteristic motion of the crop, the particulates within the crop need to be accurately identified and their movement recorded. This section outlines particle tracking methods utilizing high speed camera techniques.

Yang and Schrock (1993) established an image transformation method for determining a kernel's position in three dimensions. The kernel was dropped from a set height and the falling motion of the kernel was recorded using one high speed camera. A mirror was placed at an angle to the image plane which acted as a virtual image to allocate the third dimension of the kernel's position. The falling kernel and virtual kernel image were recorded by setting the exposure time so multiple images were superimposed on a single frame of film. The methods for processing the images on a single frame appeared relevant for tracking particle movement at low densities but because measurements of crop in a large square baler were high density measurements, this method would not be practical.

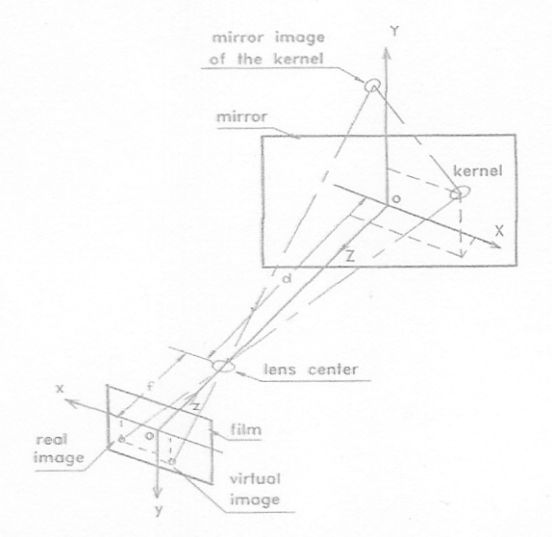

Figure 2.4: Yang and Schrock (1993) method for determining kernel's position in three dimensions. A kernel was dropped from a set height and the kernel's position was recorded using a high speed camera. A mirror was placed at an angle to the falling kernel which acted as a virtual image. Between the virtual image and the real image, the kernel's position in three dimensions could be determined.

Fiscuss et al. (1969) studied grain stream velocities for several common grain handling systems. Grain streams were filmed using a high speed camera at a rate of 2,000 to 7,000 pictures per second. Kernel speeds were compared against a grid background to determine the stream velocity. Measurements were made on the outer layers as this technique could not determine the core stream velocity, although the core velocity was assumed to be the same as the outer layers. Like grain stream measurements, only the outer layers of crop flow could be measured in a large square baler and the core velocity would be assumed to be the same. Utilizing a grid background is a simplistic approach to determine the kernel's motion compared to the sophisticated technology available today, although it provides fundamental results for determining the motion of the grain.

Karayel et al. (2006) investigated seed spacing and velocity of fall for seed distribution from a coulter outlet of a seed drill. Measurements were conducted using a digital high speed camera at a rate of 750 frames per second. Analysis of the images was performed using Optimus version 6.2 software (Media Cybernetics, Silver Springs, MD). A reference line was drawn on the images and the average velocity of fall was determined by comparing the distance the seed traveled relative to the reference line within 20 frames from the seed leaving the coulter outlet.

Similar to the research by Yang and Schrock (1993), measurements were based on low spatial density. These methods would not be practical for measuring high density crop flow in a large square baler unless an external entity was added to distinguish the movement. A noteworthy difference between the similar studies of Karayel et al. (2006) and Yang and Schrock (1993) was the technology incorporated in the experiments as Karayel et al. (2006) used software to locate the movement of individual seeds. Even within the last 10-15 years, imaging technology has rapidly evolved, increasing the researchers' ability to further exploit and quantify particle motion using imagery.

Cointault et al. (2003) analyzed the physics of fertilizer spatial distribution from a centrifugal spreader utilizing a high-resolution, low-cost imaging system. The imaging system operated by timing a sequence of flashes for multiple exposures on a single frame. The images there were analyzed using several techniques to estimate the trajectory of fertilizer granules as initially ejected from the spreader mechanisms. Incorporating a similar high-resolution imaging system to measure the crop flow in a large square baler would be advantageous to accurately identify the particulate of crop, although, a multiple exposure image would not be possible without utilizing tracers to identify particular points within the crop.

Numerous researchers have utilized advanced high-spatial density measurements such as Optical Flow and Particle Image Velocimetry (PIV) techniques to analyze flow patterns, although were not utilized in this study due to the complexity. Estimating the crop movement before employing a more complex method provides a solid base for further refinements.

2.3.1. Tracers

In some instances, tracers are inserted to aid in distinguishing the movement of the medium. Using tracers and high speed imaging provides several advantages and disadvantages. One advantage is that the measurements are non-intrusive. Velocity measurement can also be determined over the whole field of view rather than at a singular point. On the other hand, if the flow is seeded with tracer particles, there is an indirect measurement of velocity as the measurements are recorded following the tracers themselves and not the mediums' density under study. Hence, measurements require the experimenter to carefully check each experiment to

determine if the tracer's motion faithfully follows the medium under inspection, at least to the degree required by the objectives. Smaller tracers will follow the medium better, as there is less induced velocity lag (Raffel et al. 1998).

2.4. Pressure-density Relationship

The pressure-density relationship investigates the density of crop in relation to the reaction force upon compression. This study focused on the trajectory of crop leaving the precompression room into the bale chamber, and the pressure-density relationship facilitated predicting the density before the crop was forced through the bale chamber.

In an ideal study, comparison of top/bottom flake densities would involve sampling flakes immediately after being compressed by the plunger. The sampled flake would be removed from the bale chamber, divided into top and bottom halves and then each half weighed. Assuming each half to be of similar volume upon compression, the weights would indicate the density variation between the top and bottom halves of every flake. In practice, this method would not be possible unless extreme modifications were made to allow access into the bale chamber. Also, the obtainable accuracy of cutting straw into equally based halves was questionable.

In need of a better process to evaluate top and bottom flake densities, the pressure-density relationship was referred to for investigating density differences during crop compaction. When the crop is compressed by the plunger, the air voids within the crop become smaller as the plunger pushes rearward. The air voids become smaller because solid crop matter is pushed into the voids and by definition, the density increases. Increased solid matter causes the reaction force opposing the plunger's motion to increase and hence, the pressure-density relationship of crop compression exists.

The pressure-density relationship is fundamental for compression of crop although representing this process can be difficult. The compression process has been investigated by numerous researchers although the techniques they employed varied. The difficulty in modeling the pressure-density relationship is due to variability of the crop material and the complexity of the compression process.

Studies by Skalweit (in Kanafojski and Karwowski 1976) investigated the compression of crop in a laboratory pressure vessel. Skalweit (in Kanafojski and Karwowski 1976) assumed that at low compression speeds, the pressure-density relationship could be expressed using the polytropic gas equation. Based on this assumption, the plunger's specific pressure was expressed as:

$$p = c\rho^{m_e}, \tag{2.1}$$

where:

p = pressure acting on the plunger (Pa),

ρ = density of compressed hay (kg/m^3) and

c and m_e = experimental coefficients.

Equation 2.1 was developed based on straw of specific moisture content and did not consider; compression of other materials, varying moisture content or speed at which the material was crushed. These shortcomings were later analyzed by Sacht (in Kanafojski and Karwowski 1976).

Sacht's (in Kanafojski and Karwowski 1976) research indicated that for wheat straw, oat straw, alfalfa hay and grass hay, Skalweit's (in Kanafojski and Karwowski 1976) polytropic model was generally valid for a crushing range up to approximately 2 MPa. Table 2.1 outlines approximate coefficient values for c and m found by Sacht (in Kanafojski and Karwowski 1976) although these values are valid for dry materials only.

Table 2.1 Coefficients for c and m outlined by Sacht (Kanafojski & Karwowski 1976).

Pressure Range (kPa)	Values	Wheat Straw 89% dry mass	Oat Straw 88.5% dry mass	Alfalfa Hay 83.5% dry mass	Meadow Hay 86% dry mass
150 to 500	c	$2.53*10^{-3}$	$9.80*10^{-4}$	$3.70*10^{-4}$	$6.75*10^{-5}$
	m	1.47	1.59	1.69	1.96
500 to 2000	c	$2.78*10^{-4}$	$1.56*10^{-5}$	$1.78*10^{-6}$	$8.55*10^{-7}$
	m	1.89	2.35	2.64	2.73

Moisture content affects the resulting pressure to crush the crop because moist crop has a tendency to bend when compressed, whereas dry crop has a tendency to become brittle and break. Continued laboratory investigations by Sacht (in Kanafojski and Karwowski 1976), determined the following relations for alfalfa:

$$p = \frac{7.5 \cdot 10^{-6}}{W} \rho^{2.10}, \tag{2.2}$$

and meadow grass:

$$p = \frac{5.0 \cdot 10^{-6}}{W} \rho^{2.49}, \tag{2.3}$$

where:

W = moisture content dry basis (between 15-55% only).

Equations 2.2 and 2.3 are valid for pressure ranges between 200-1500 kPa. Both moisture and pressure ranges are within normally encountered ranges as seen during baler operation (Kanafojski and Karwowski 1976). If the moisture content of the crop is too high during harvest (baling of crop), compacted crop will begin to heat and potentially self combust.

Uziak (1989) compared four different representations of pressure-density relationships during the dynamic analysis of a pressing system. Research by Mewes (in Uziak 1989) developed a modified version of Skalweit's (Uziak 1989) polytropic relationship,

$$p = b(\rho - \rho_0)^n, \tag{2.4}$$

where:

ρ_0 = density of hay before being compressed by plunger (kg/m^3) and

b and n = experimental coefficients.

Mewes' (in Uziak 1989) relation was limited to low pressure ranges (<<1 MPa).

Osobov (in Uziak 1989) assumed the degree of compression to be a linear function of pressure and an increase in pressure rise at any location within the material would depend on the degree of compression. The resulting equation obtained was of the form:

$$p = \frac{C}{a}\left(\exp\left[a(\rho - \rho_o\right] - 1\right), \tag{2.5}$$

where:

C and a = experimental factors.

Studies conducted by Chrapacz (in Uziak 1989) resulted in the following expression:

$$p = 1.92 \cdot 10^{-5}\, \rho^{2.178} \alpha \beta K\,, \tag{2.6}$$

where:

$$\alpha = 1 - 0.02(W - 15.3)\,, \tag{2.7}$$

$$\beta = (0.084v)^{2.75}\,, \tag{2.8}$$

v = velocity of compression (m/s) and

K = coefficient depending on the material state (dimensionless).

Equations 2.1 and 2.4 through 2.6 were used for Uziak's (1989) analysis. The results from the analysis were based on calculating the coefficient of speed fluctuation for several combinations of input parameters (no field tests were performed). Calculations were done based on an Agromet Z-225 baler produced in Lublin, Poland and all calculated values were determined from correlations.

Uziak (1989) found that the different forms of equations minimally affected resulting coefficient of speed fluctuation. Skalweit's (in Uziak 1989) expression had the largest coefficient of speed fluctuation whereas Osobov's (in Uziak 1989) formula produced the smallest coefficient of speed fluctuation. Uziak (1989) recommended using a formula of the simplest mathematical form to calculate coefficient of speed fluctuation (e.g. Skalweit's (in Uziak 1989) or Mewes' (in

Uziak 1989) formula) because the coefficient was found to be nearly independent of the equation form.

Srivastava et al. (1993) described the resultant density during baling as being dependent on the type of material being baled, moisture content of the material and resistance provided by the converging walls of the compression chamber. As the material moves through the compression chamber, the convergence of the walls (assuming only two walls converge) causes the crop to compress laterally. Assuming the crop material is elastic, the force acting on the plunger was expressed as

$$F = \frac{E_h y_c}{d} Lwf_h \tag{2.9}$$

where:

F = force applied by plunger (N),

E_h = effective modulus of elasticity of crop material (kPa),

L = length of converging section (m),

y_c = total convergence in converging section (mm),

d = compression chamber depth (m),

w = width of compression chamber (m) and

f_h = coefficient of friction between crop and bale chamber.

In practice, the above relation is difficult to solve due to the challenges in determining values for E_h, although the equation provides valuable insight into the problems of density control. As the moisture content of the crop changes, both E_h and f_h change causing the plunger pressures and resulting bale densities to change.

Until now, the literature reviewed focused on the pressure-density relationship of laboratory pressure vessels or small square balers. These equations cannot be directly applied to pressure-

density relationships within large square balers as the equations were defined for different applications. The equations for the small square baler cannot be employed because of the large size difference between bale chambers and also, the bale chamber has three moving walls on a large square baler compared to one or two moving walls on a small square baler. The moving bale chamber wall(s) rotate about a pivot and apply a force to the sides of the bale. The mechanisms used to apply this force were usually a hydraulically controlled linear actuator or a spring.

Shinners et al. (2000) investigated several evaluation techniques for measuring the volumetric or mass flow rate in a John Deere model 100 large square baler. One effort was to correlate the plunger force with volumetric flow rates using force sensors mounted on each side of the plunger gearbox. Output values from the force sensors were compared to the volumetric and mass flow rates by two theories: 1) mass flow rate would be proportional to the integrated or average force from the load cells; or 2) mass flow rate would be proportional to width of impulse spike during compression.

The resulting measurements did not correlate well with the volumetric or mass flow rates. The integrated or net average force measurements had correlation levels correlated less than 60% in alfalfa and 40% in straw. The pulse width force measurements scored slightly higher, although correlation values were less than 70% for alfalfa and 40% for straw. There was no regression model for net average plunger force in wheat straw because the model was not significant ($p < 0.05$).

Inclusion of the plunger crank speed sensor increased the correlation of the models which was most likely because of a direct relation between the plunger crank velocity and force acting on the plunger. If a larger wad of crop was ejected into the compression chamber, the plunger speed was reduced due to a larger force spike. Shinners et al. (2000) recommended the multi-parameter model should include chamber wall pressure as an added variable.

Klenin et al. (1970) described the compression process of crop material being compacted by the plunger as illustrated in Figure 2.5. Initially at point O, the plunger is in its most forward

position hence is not in contact with any crop and the acting plunger pressure is zero. The plunger moves rearward and does not come into contact with crop until reaching point A. Typically a plunger stroke is approximately 25-30% greater than the width of the wad of crop. The plunger compresses the crop to point B where the plunger comes in full contact with the crop and applies pressure to the entire mass. Once at point B, the plunger pressure continues to increase over the entire mass indicated by line BC. Upon reaching point C, the plunger reaches a maximum pressure and overcomes static friction to push the bale rearward in the compression chamber (line CD). During this period of movement, the pressure remains constant (P_2 = CD). The elastic properties of the compressed crop cause the bale to springs back against the plunger as the plunger retreats from its furthest extended stroke. The crop spring back until point E, at this point, the crop becomes held by the hay dogs which prevent the compressed crop from springing back and losing compaction pressure. Hence, the pressure applied to the plunger rapidly drops to zero (line EF).

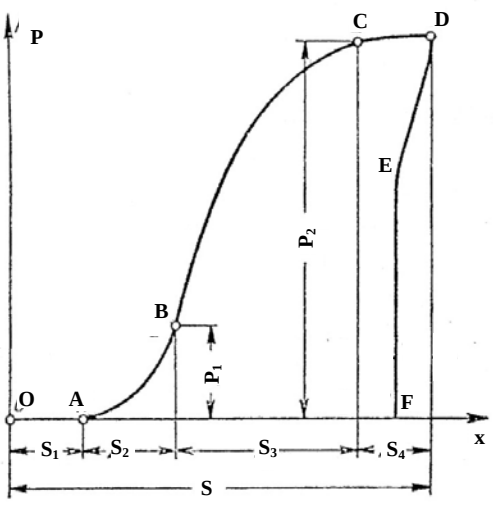

Figure 2.5 Applied plunger pressure, P, vs. plunger position, x, for one complete plunger cycle (Klenin et al. 1970)

2.5. Controller Area Network

The Controller Area Network (CAN) is a digital protocol for electrical communications and is an industry standard for agricultural equipment manufacturers. The CAN interface is between the central processor unit (CPU) and sensors/receivers on the baler. The objective of the CAN is to reduce the number of dedicated lines (parallel interface) by using a sophisticated on-board network bus (serial interface).

CAN signals were of importance as these digital signals were recorded to monitor the operation of the baler during field experiments. From the CAN, knotter engagement, stuffer engagement, plunger position, PTO speed, relative load acting on the plunger and the hydraulic pressure acting on the bale chamber walls could all be determined from monitoring the CAN.

The CAN signals were composed of frames. On a CAN network, 4 different types of frames can be conveyed: data frame, remote frame, error frame and overload frame. The frame of interest was the data frame. The data frame was composed of seven fields as shown in Figure 2.6: start of frame (SOF), arbitration field, control field, data field, cycle redundancy check (CRC) field, acknowledgement field and end of frame field. Depending on the type of CAN used, the arbitration field is either 11 bits (CAN 2.0A) or 29 bits (CAN 2.0B). The data field can contain up to 8 bytes of information and withholds the data the device is relaying.

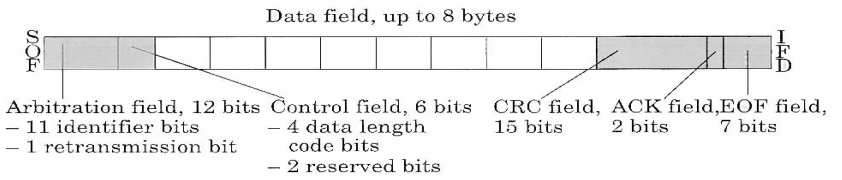

Figure 2.6 Typical CAN data frame (Pop et al. 2004)

The data frames require a conversion from either raw binary or hex values to a recognizable form. The binary or hex values are converted to decimal values and then a scaling factor, offset and units are applied to produce a value that is identifiable to the user (National Instruments 2005; Pop et al. 2004; Zurawski 2006; Lindenburg 2004).

3. OBJECTIVES

The goal of this study was to analyze the potential change in densities caused during crop trajectory from precompression room to compression chamber in a large square baler. This study concentrated on comparing densities in the top and bottom halves of each bale with respect to maintaining uniform density between these regions. To achieve the ambitions outlined above, the objectives have been separated into two main experiments; measuring crop trajectory and measuring pressures at the top and bottom of the plunger. The following two sections describe in further detail the objectives for these two cases.

3.1. Measuring Crop Trajectory

The projectile motion of the wad of crop being ejected from the precompression room to the compression chamber was filmed using a high speed camera. Understanding the motion of the crop before being compressed is essential in maintaining a final product that is uniform. The objectives for this experiment were to investigate the effects of material flow on bale density. In particular, the specific objectives for this study were to:

- measure crop displacement, as a function of time, during transfer from the precompression room to the compression chamber before being compressed into a flake,
- determine crop velocity and acceleration based on displacement-time data, and
- compare crop strain in the top and bottom portions of the ejected wads of crop.

3.2. Measuring Plunger Pressure Top/Bottom

Plunger pressures were measured in top and bottom locations as a means to validate the results from the crop trajectory measurements and develop a broader comprehension of possible density changes occurring while forming the bale. Ideally, immediately after a wad of crop was ejected,

the wad of crop would be split into two halves (top and bottom) and the mass of each half would be determined. From the measured weights, the density of the top and bottom halves of each wad of crop could be compared. However, in practice, cutting the crop into two evenly split sections is very difficult to accomplish without introducing large amounts of error. Hence, plunger pressures were measured to compare top and bottom densities, knowing that pressure is directly related to crop density. The objectives for measuring plunger pressures were to:

- statistically compare the means of peak top and peak bottom plunger pressures,
- develop pressure profiles for plunger pressure (top/bottom) versus plunger displacement using governed settings, and
- develop a model to determine the difference in final bale mass (top/bottom) based on measured parameters, difference in bale mass and equipment settings used.

4. MATERIAL AND METHODS

4.1. Filming From Side

In order to film inside the large square baler, several modifications to the baler were needed. The first stage of modifications was to remove the side panel to allow space for filming equipment and access to the side of the baler for cutting viewing windows. Both top and bottom plunger rails were reinforced, then the viewing areas were cut into the side of the baler. Safety glass was incorporated to enclose the cut out areas and paint was used to differentiate between the moving plunger (fluorescent orange) and the outside viewing area (flat black). The viewing windows are illustrated in Figure 4.1.

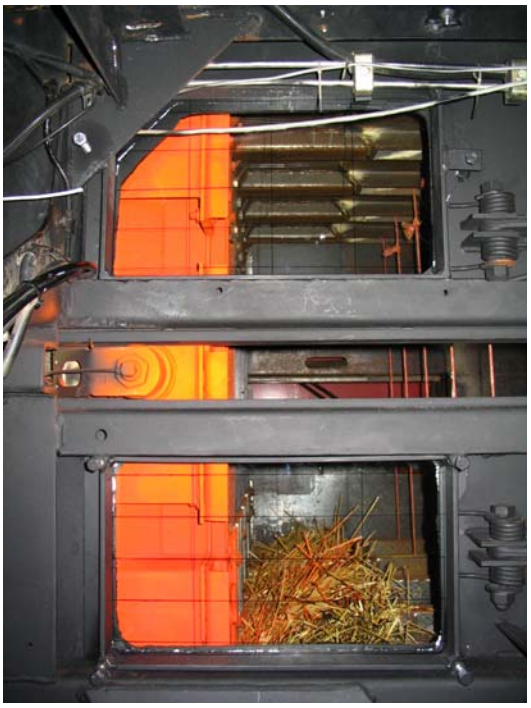

Figure 4.1 View of windows cut into side of the baler for measuring crop motion.

To accommodate the filming process, a sturdy mount was developed. The mount was situated on the left side of the machine, bolted directly to the side panel mounts. The apparatus supported both the high speed camera (HSC) and the digital video camera (DVC). The mount had three degrees of linear movement for positioning the HSC and independent positioning for the DVC. Figure 4.2 illustrates the camera mount for the side of the machine.

Figure 4.2 Side camera mount used for filming crop flow from the side of the baler.

The baler's twine boxes were incorporated in the side panels of the machine, and because one side panel was removed, modifications were required to retrofit the twine housing and routing. Figure 4.3 shows the modified baler with the side panel removed, the compartment installed for data logging equipment, the HSC mount and the rerouted twine.

Figure 4.3 Illustration of modified baler; side panel removed, camera mount installed, twine rerouted and compartment used for logging equipment.

Plastic milk crates were used to house the twine and the rerouting of twine was accomplished by using steel loops welded to the side of the baler. The twine was routed through electrical

conduit near moving components (i.e. above plunger) to prevent entanglement. A plastic container was also mounted on the side of the machine to enclose the video-capture equipment and miscellaneous tools.

To achieve the lighting requirements for high speed imaging, the baler was fitted with four narrow halogen lights and two halogen spotlights. The narrow halogen lights were fitted in between the plunger rails as shown in Figure 4.4 and the halogen spotlights were fitted on the side of the camera mount as shown in Figure 4.5.

Figure 4.4 Four narrow halogen lights installed between the plunger rails.

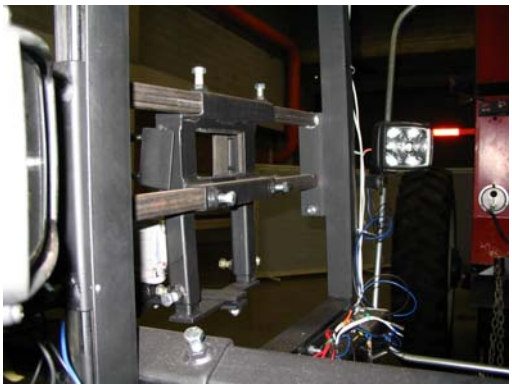

Figure 4.5 Two halogen spotlights installed on the side of the HSC mount.

Due to problems with glare from external light, the baler was covered with a tarpaulin. The tarpaulin prevented light from entering around the camera apparatus and also light from entering through cracks inside the bale chamber which proved to be a problem. In order to keep the tarpaulin away from moving components, metal bars were used to provide the framework over which the tarpaulin was draped. Figure 4.6 illustrates the baler covered and ready for field tests.

Figure 4.6 Baler tarped and prepared for field tests.

4.2. Measuring Plunger Pressures

Plunger pressures were measured in both top and bottom locations. Measurements were taken in both North American and European conditions with different configurations in each region; in North America, four pressure sensors were used and in Europe, two pressure sensors were used. Duplicate pressure sensors were used in North America to act as a backup in the event of a failed sensor and also, to compare between left and center plunger pressures. Figure 4.7 and Figure 4.8 illustrate the pressure sensor locations for European and North American configurations, respectively.

Figure 4.7 Configuration of the sensors mounted on the plunger for experiments performed in Europe.

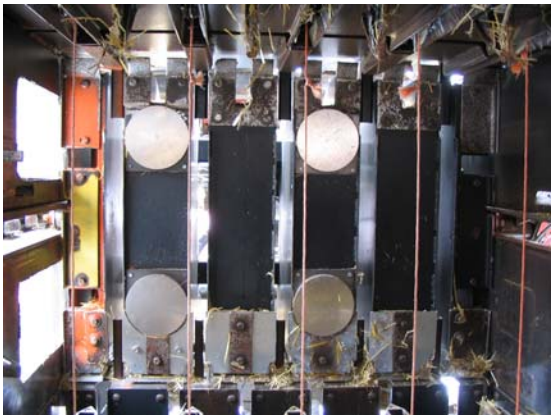

Figure 4.8 Configuration of the sensors mounted on the plunger for experiments performed in North America.

The balers used in North America and Europe were similar with the only appreciable difference being that the baler used in North America was a five-string baler (BB960) and the baler used in Europe was a six-string baler (BB960A). Both plungers were of the same width and height although the geometry used to construct each plunger was different to account for the different number of strings. Due to this difference in construction, different pressure sensors were fabricated for the BB960 and BB960A. The overall sensor diameter used for the BB960 was 165.1 mm (6.5") and for the BB960A, 114.3 mm (4.5").

The pressure sensors used a diaphragm pressure transducer design as shown in Figure 4.10. In designing the sensors, the assumed maximum pressure to be measured was 500 kPa and the maximum design stress employed (using stainless steel 316) was 205 MPa. The sensors were designed with a 12.7-mm (1/4") supporting ring leaving 152.4-mm (6") and 101.6-mm (4") of material for the center diaphragms. The calculated thicknesses of the diaphragms (assuming a Poisson's ratio of 0.28) were 2.77 mm (0.109") for the smaller sensors used in Europe (BB960A) and 4.17 mm (0.164") for the larger sensors used in North America (BB960). Sample calculations for determining diaphragm thickness can be found in Appendix A.

In order to implement the pressure sensors, several steps were required. The sensors were manufactured by turning stock material in a lathe to the required dimensions. Four strain gages were then installed on each sensor with two active gages and two dummy gages for temperature compensation. The dummy gages were mounted on the same material and separated from the sensing diaphragm to prevent induced strains during operation. The gages were configured in a Wheatstone bridge with one active gage in tension and the other active gage in compression. Figure 4.10 illustrates one of the manufactured pressure sensors.

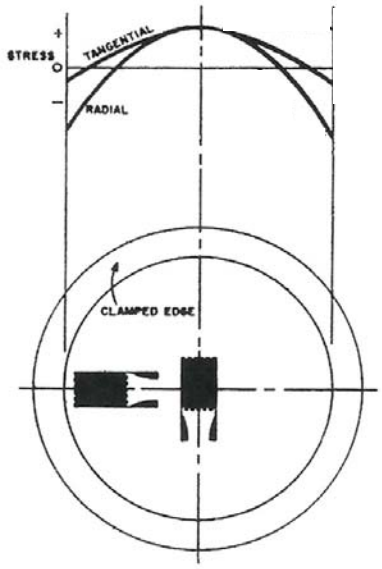

Figure 4.9 Diaphragm pressure sensor design illustrating stress distribution for uniformly loaded diaphragm and clamped edges (Mitchell 1983).

Figure 4.10 Fabricated pressure sensor used to measure plunger pressures. Two active strain gages were mounted as shown in the center and right of the sensor. Two dummy gages were used for temperature compensation as shown in the top left of the sensor.

The plunger's wear plates were modified to function as backing plates for the pressure sensors. The backing plates were secured to the plunger using the fasteners for the original wear plates and self tapping screws. The sensors were positioned on the plunger with the top sensor(s) being centered in the top half of the plunger's face and bottom sensor(s) centered in the bottom half of the plunger's face.

The strain gages were powered and their signals were amplified and recorded using a signal conditioner connected to a USB-1608FS data logger (Measurement Computing, Norton, MA). The signal conditioner excited the bridge with a ±5 volt supply and amplified the output from the bridge. The data logger digitized the analog output from the signal conditioner and recorded the data to file on a laptop. The data logger had 16-bit resolution and recorded at the set rate of 250 samples per second (S/s). The signal conditioner, data logger and laptop were located inside the tractor cab to protect these devices and to provide safe access during operation. An additional channel on the data logger was used to record a magnetic reed sensor which registered the plunger's most forward position during each complete plunger stroke.

Figure 4.11 illustrates calibration of load cells in North America and Figure 4.12 illustrates calibration of load cells in Europe. The method for calibrating the pressure sensors involved removing the sensors from the baler and applying a load in a laboratory compression tester. The sensors were positioned on the bed of the compression tester with the backing plates down and the sensor's face aligned with the head of the compression tester. Once aligned, a medium was placed between the pressure sensor and the laboratory compression tester. Foam was used as a medium for calibrations in North America whereas a matt of grass was used for calibrations in Europe. The pressure sensors were configured for calibration using the same equipment and settings (gain and offset) as used in field applications; signal conditioner, data logger and laptop. A force was applied to the sensor and the output was recorded to file for fixed loading intervals. The force applied by the compression tested was translated to pressure by dividing the applied force by the area of the pressure sensor diaphragm. The resulting voltage output of each sensor was used to develop calibration equations, relating pressure to output voltage.

Figure 4.11 Calibration of pressure sensors using a laboratory compression tester (North America).

Figure 4.12 Calibration of pressure sensors using a laboratory compression tester (Europe).

During field operation, CAN signals (see Section 3.4) were recorded to monitor chamber wall pressures (ChamPress), percent load (PLoad), stuffer ratio (StuffR) and knotter operation. Logging of CAN signals involved connecting to the CAN bus and recording the signals with a

laptop by use of a PCMCIA CAN card. For field tests in Europe, the CAN signals were recorded at the same rate as the data logger (250 samples/second (S/s)), whereas in North America, the CAN signals were recorded each time the CAN bus changed state. For North American data, the recorded CAN signals required timing with the recorded data logger data. Details of timing CAN data with data logger data are outlined in Section 5.2.1.

When performing field tests for pressure measurements, several courses of action were taken. First, considerations were made to start a new bale. In North America, the baler's knotter trip was set to produce a short bale causing the knotters to engage early in the run. The knotter engagement indicated the start of a new bale and the engagement was recorded by the CAN logger. The knotter trip on the baler in Europe could be activated from the cab of the tractor and was manually initiated by the operator at the beginning of the run. Once knotter engagement was taken into account, the baler was situated in front of a windrow and the power take off (PTO) activated. The PTO speed was carefully set to 1000 RPM and then the logging systems were started. The data logger was started first then the CAN logger was started. With both loggers operating, the baler was set into motion. The first knotter cycle was observed and baling continued until the second knotter cycle. At the point of the second knotter cycle (bale complete), the CAN logger was stopped then the data logger was stopped. Both logger files were saved utilizing the run or bale number as a standard file name. The bale was then labeled for future bale weight measurements. Each bale was approximately 1.83 to 2.44 m (6 to 8 ft) long.

The collection of data in Europe was organized by randomizing the settings used. For North American data, only one setting was used (medium flake size and 80% constant density) hence, randomization was not required. Table 4.1 defines the flake size in relation to corresponding baler adjustment.

Table 4.1: Flake size and corresponding baler adjustment

Flake Size	Baler Adjustment - Flake
Thin	1/10
Medium	4/10
Thick	8/10

4.3. Measuring Bale Weights

After measuring plunger pressures, the bale weights were then examined. Due to known problems with trying to split the bale into top and bottom sections, each bale was weighed without cutting. The concept for weighing the bales is illustrated in Figure 4.13. Each bale was turned on its side and the forces F_{Bottom}, F_{Top} and weight total (WT) (see Figure 4.13) were determined. Differences in F_{Top} and F_{Bottom} indicated a difference in crop densities in the top and bottom halves of the bale, assuming the top and bottom sides were parallel.

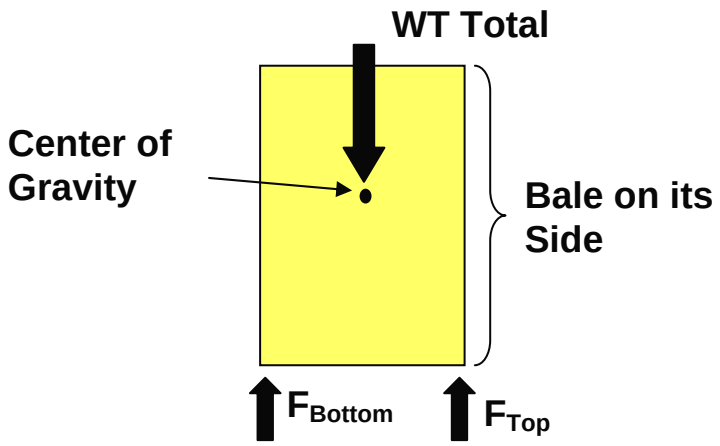

Figure 4.13 Free Body Diagram (FBD) for measuring bale weights

The scale used in Europe is illustrated in Figure 4.15. A tractor equipped with hydraulics and a 3-point hitch was used to operate the scale. The bale was first tipped on its side then the arms of the scale were opened and the tractor/scale unit was backed over the bale. The arms of the scale were then squeezed down onto the bottom of the bale utilizing the hydraulics of the tractor and the bale was then lifted. Each arm on the scale was instrumented for force measurement and once elevated, F_{Bottom} and F_{Top} were measured. Each bale was measured twice, once from each end of the bale and the two measurements were averaged to determine the final measured value.

The scale used in North America (Figure 4.16) was designed to determine the same forces (F_{Bottom} and F_{Top}) as the scale in Europe although operations for determining these forces were rather different. The concept for the North American scale was to place the bale onto a level platform and weigh each side of the bale on the platform. The bale was placed on the platform

by first tipping the bale on its side and then using a tractor equipped with a front end-loader to position the bale on the platform. The level platform was free rotating on one side (one degree of freedom) and was supported on the other by a load cell. The bale was positioned on the platform with one side of the bale pushed tight against a wooden board. The inside face of the wooden board was aligned with the platform's axis of rotation. The purpose of the wooden board was to ensure each bale was weighed at the same location and the weight of the opposing side of the bale could easily be determined by summing the moments about the axis of the platform. Figure 4.14 illustrates a schematic of the scale used to measure bale weights in North America.

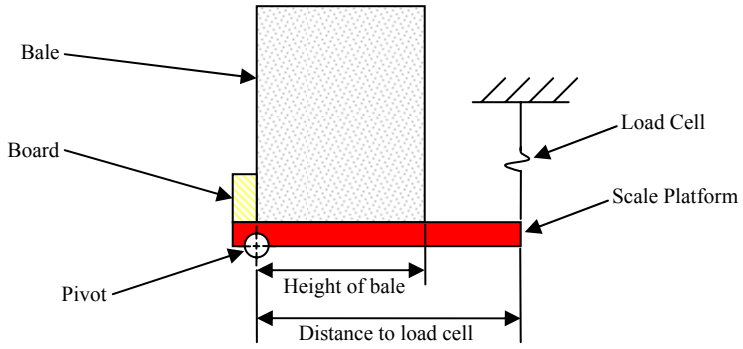

Figure 4.14: Schematic of scale used to measure bale weights in North America.

For convenient access to position the bales on the platform, the load cell was located at a distance away from the positioned bale. Each bale was weighed twice, once with the top of the bale against the scale platform and once with the bottom of the bale against the scale platform. The total weight (WT total) was also measured by suspending the entire bale from a load cell. From these measured parameters, F_{Top} and F_{Bottom} were calculated twice for each time the bale was placed on the scale (see Appendix A: Sample Calculations). These two replicate values ($F_{Top(1)}$ and $F_{Top(2)}$, and $F_{Bottom(1)}$ and $F_{Bottom(2)}$) were averaged to determine the final measured values. For further information, sample calculations for the determination of F_{Top} and F_{Bottom} are illustrated in Appendix A.

Figure 4.15 Illustration of the scale used for experiments performed in Europe.

Figure 4.16 Illustration of the scale used for experiments performed in North America.

4.4. Location of Field Measurements

Data were collected in two locations; Issoudun, Département de l'Indre, Région du Centre, France and Dundurn, Saskatchewan, Canada. Video data were only collected in North America whereas pressure data were collected in both North America and Europe. All data were collected with wheat straw tailings from rotary combines.

Pressure data in Europe were collected on August 23-24, 2004 and from these measurements, a total of 20 bales were analyzed. Of the 20 bales, six different settings were used; 2 different wall pressures (7 and 11 MPa) and 3 different flake settings (thin, medium and thick flake). A summary of the settings used and measured parameters are listed in Appendix B.

Pressure data in North America were collected on October 10, 2004 and video data were collected on October 10 & 12, 2004. For pressure measurements, a total of 9 bales were used for analysis and all 9 bales were formed using 80% constant density and a medium flake setting (refer to bales 1-9, Table B1, Appendix B). Filming from the side of the machine was done on October 12, 2004. All video measurements were taken using the medium flake setting. Further details of the settings and measured parameters are listed in Appendix B.

5. DATA ANALYSIS

5.1. Video Analysis

Analysis of the videos involved several processes to obtain results from the recorded crop trajectories. This section outlines the processes used to analyze the recorded videos and builds the basis for the presented results. Numerous macros were used to perform specific tasks on the data sets and whenever possible, the task is referred to by the specific macro name. Further information regarding the use of specific macros can be found in the accompanying CD (see Appendix E).

5.1.1. Extraction of Frames From Video

The first step in the analysis required the videos to be converted into a usable form. In this case, the high speed videos were stored as audio video interleave (.avi) format and required each frame of the video to be extracted. The frames of each video were extracted using specialized software and each frame was stored either in jpeg or bitmap format. At a frame rate of 250 frames per second and a maximum recording time of 8 seconds, there were approximately 2000 stored images for every recorded video.

The videos filmed from the side of the baler were recorded with the camera rotated at 90°. For convenience purposes, the extracted frames were rotated so the images would show the crop trajectory acting upwards, as one would expect. The extracted frames were rotated by using software to batch convert the stored images.

5.1.2. Particle Tracking Software

Before the stored frames could be analyzed, software was required to assist in plotting the projectile motion of each wad of crop. This section outlines the methods taken to utilize and setup software for monitoring each wad of crop's position when ejected from the precompession room into the compression chamber.

The software used for analysis was AutoCAD™ (AutoDesk AutoCAD, 2004) combined with macros written in Visual Basic. The steps to setup this software included importing an image,

scaling the image and then setting a coordinate system for use throughout the analysis. The image was imported then scaled based on known measurements for the chamber geometry. The coordinate system was positioned with the origin located at the bottom left-hand corner of the bottom viewing window. The scaling factor and dimensions for locating the origin were documented for use throughout the study.

Macros were written to perform a rapid series of events in AutoCAD and were used to assist in analysis of the images. A macro was designed to insert three images into the CAD drawing at defined positions (side by side) and scaled to the proper dimensions. Before the images were inserted, the macro prompted the user to input the first image number, then inserted three sequential images which were referred to as before, current and after views, from left to right, respectively.

With the three views inserted into the drawing window, lines were superimposed on the images to delineate the boundary layers of the windows and partition the viewing windows into four regions. The regions were created by splitting the top and bottom viewing windows in half. Referring to Figure 5.1, the regions were labeled with the uppermost being Region 1 and Regions 2 through 4 following below.

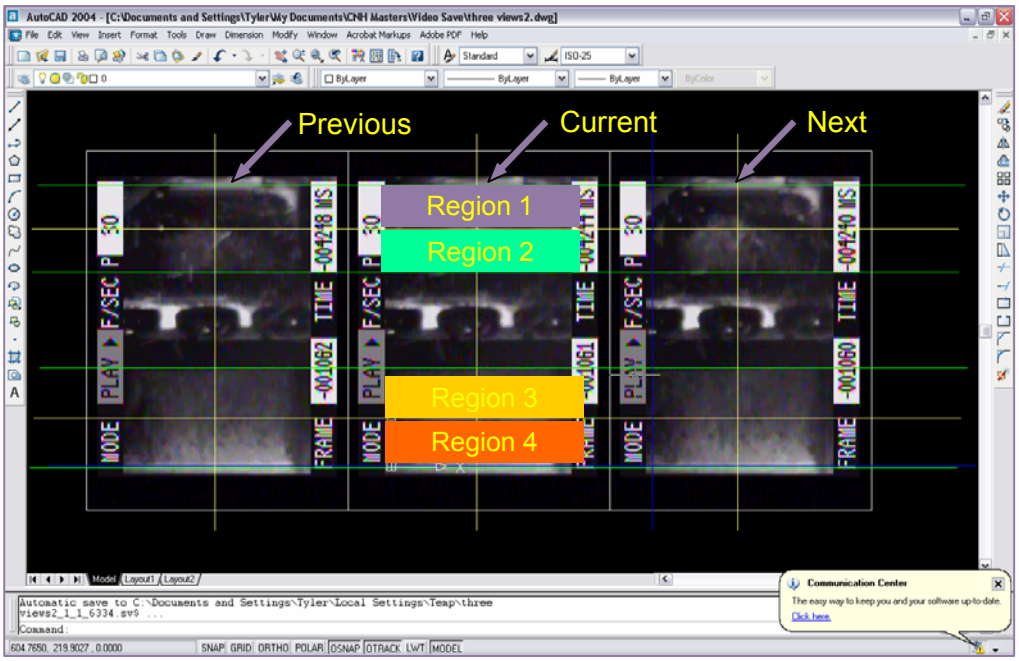

Figure 5.1 Illustration of method used in AutoCAD for tracing particle motion. Three views were inserted to allow comparison between the previous and following frames. The current frame illustrates the four divided regions.

Once the images were set up in a CAD drawing, macros were written to advance and retract the images in relation to time. Two macros were used to advance and retract the images,. When either macro was activated, each image would be advanced by one frame or retracted by one frame. The videos were recorded at 250 frames per second, so each advancement or retraction of a frame would represent an increment of 4 ms (1/250 s). By cycling through the series of images, the projectile motion of the crop could be monitored in the drawing window of AutoCAD.

To track the crop flow, a series of points were inserted and the coordinates of the points were stored to file. Three macros were written to verify the data, write data to file and delete the system of data points. A macro counted the number of points in the drawing window and displayed the result in a text box. By comparing the resulting number of points to the difference between the first and last frame number, the macro ensured no frame was missed. If there were no frames missed, another macro was used to export the coordinates of each point in the drawing window to a text file. The contents of the text file could then be imported into Microsoft Excel (Microsoft Corporation, Redmond, WA). After the data points were written to

file, a macro was used to remove the data points in the CAD drawing to prepare for the next region or wad of crop to be analyzed.

A summary of the macros used is provided in Appendix E and the AutoCAD files/macros are stored on the companion CD. See file Read_Me.txt on the companion CD for more information to access these files.

5.1.3. Analysis of Images

For each recorded wad of crop, a standard procedure was followed to ensure each video was analyzed consistently. This section outlines the procedure followed for tracking the projectile motion of each wad of crop.

The starting frame was determined first and was critical because uncertainty would shift the results forward or backwards in relation to time. Before the images were inserted into AutoCAD, each file was manually inspected to determine the number of wad of crop recorded and the approximate beginning frame number of each recorded wad of crop. The frame number along with the associated file name was noted and readily available for the analysis. A macro was executed to input the beginning frame number and import the three views of the crop into the drawing window. The images were advanced using a macro until the plunger's face reached the center of the current viewing window. Once positioned in the center, the images were retracted 10 frames (40 ms) and this frame was referred to as the start frame for the analysis. The images were retracted by 10 frames because this allowed for more crop material to be viewed within the windows and allowed for better selection upon the start of the experiment.

At the start frame, particles were traced back from each defined region to the bottom edge of the viewing windows. The analysis was initiated by placing a point over an identifiable or distinguished particle near the center of Region 1 using the CAD point tool. The images were then drawn back one frame using a macro. Drawing back the images one frame allowed for the process to be repeated again with a new image in the current view. The new current view was compared to the previous image using indicating lines which highlighted the previous point selected. A concerted effort was made to select exactly the same particle on the new image.

This process was continued until the particle was tracked back to the bottom edge of the window.

Once the selected particle was traced back to the edge of the window, the series of checking the data, writing the data and deleting the data was performed. Before the data were written to file, a macro was executed to compare the number of data points to the frame number. The macro would return the number of data points in the drawing and should match the beginning frame number minus the current frame number plus one. If data points and frame numbers were in agreement, the coordinates of each data point were written to a text file using a second macro. After the data were written to file, the data file was opened and the contents imported to an Excel spreadsheet. Once the data from Region 1 were safely stored, the content of the text file was cleared and the points in the CAD drawing were deleted using another macro. Finally, the image in the current view was advanced back to the start frame. These steps stored the data and prepared to repeat the analysis by tracking particles from regions 2, 3 and 4.

When the analysis of the wad of crop was complete, a new crop image was inserted into the CAD drawing. The three images on the screen were deleted and a macro was executed to reinstall three new views from the next wad of crop. If the wad of crop was stored in the same folder, the approximate beginning frame number of the new wad of crop was input when requested by the macro and the images from the new wad of crop were inserted into the drawing window. If the wad of crop was stored in a different folder from the previously analyzed wad of crop, directory paths were updated before the new wad of crop was inserted.

With analysis of each wad of crop complete (25 replications), the resulting data were organized by starting frame number and plotted. Figure 5.2 illustrates a plot of the vertical position in relation to frame number.

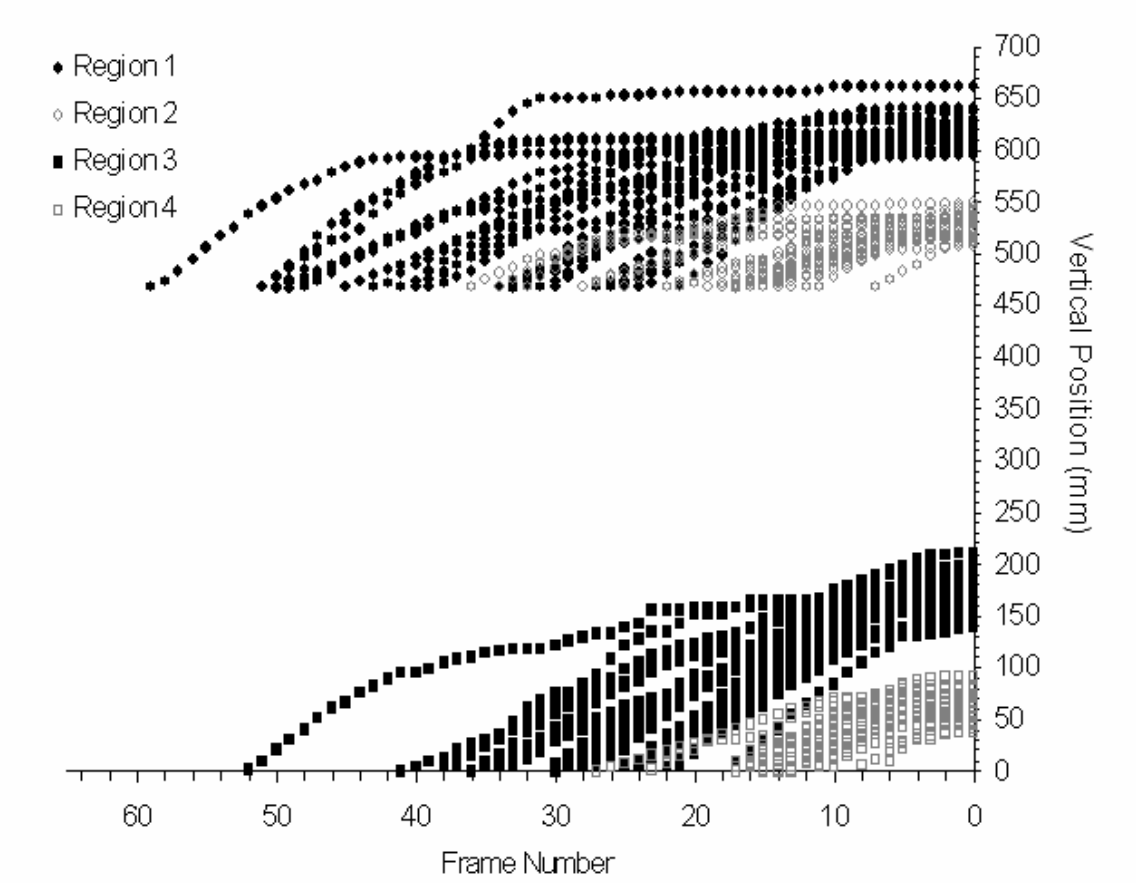

Figure 5.2 Illustration of the measured vertical displacement verses frame number for all four regions.

5.1.4. Curve Fitting

Trend lines were fitted to each region by first removing outlying data points and then fitting the data based on a second-order polynomial equation. The outliers were detected by comparing the vertical position with a confidence interval at each frame (every 4 ms). For any data point outside of this interval, the wad of crop number was recorded and the entire wad of crop was removed from the region under inspection. The 90% confidence interval for the range for each region was calculated utilizing the following equation (Weisstein 1999):

$$CI = \pm 1.64\sigma\,, \tag{5.1}$$

where:

CI = confidence interval and

σ = standard deviation of the vertical displacement calculated at each frame interval.

With the outliers removed, trend lines to describe the vertical position of the crop material, in relation to time, were determined for each region. The x-axis of Figure 5.2 was converted from frame number to time by dividing by the sampling rate and multiplying by -1. The data in each region were fitted to a second order polynomial of the form:

$$y_v = at^2 + bt + c\,, \tag{5.2}$$

where:

y_v = vertical position (mm),

t = time (ms) and

a, b and c = coefficients.

The coefficients of Equation 5.2 (a, b and c) were determined by solving the equation using three known locations. Two known locations were the starting point and end point of the crop's position. The starting point, t = 0, was when the initial particle to be tracked was selected. The particle selected was chosen to lie as close to the center of the region as possible, although assessment of this point varied from one wad of crop to the next. As such, the fitted equation should reside through the average of the initially selected points at time t = 0 (t_1, y_1). Similarly, the end point for the fitted trend should reside at the average time for the particles to reach the edge of the window, where the measurements were ended. The time and vertical position of the last measurements taken for each wad of crop were averaged to establish the second known location (t_2, y_2). The third known location was determined by identifying that at t = 0 (i.e. when plunger face was retracted 40 ms from the center of viewing windows), the vertical velocity of the wad of crop was zero ($dy_v/dt = 0$). Hence, taking the derivative of Equation 5.2 results in the third known location

$$\frac{dy_v}{dt} = 2at + b = 0 . \tag{5.3}$$

Substituting points (t_1, y_1) and (t_2, y_2) into Equation 5.2 and solving Equation 5.3 for t = 0, resulted in the determination of coefficients a, b and c for each region and the results are shown in Table 6.1. Sample calculations for determining the trend line of Region 1 are illustrated in Appendix A.

5.1.5. Calculation of Crop Strain

Crop strain was defined as the change in distance between two particles in each viewing window. If the top and bottom particles within one viewing window moved closer together, this was defined as a positive strain and if the top and bottom particles within one viewing window moved further apart, this was defined as a negative strain. Figure 5.3 illustrates a trajectory example used to clarify the procedures for determining crop strain (top and bottom) for the trajectory of one wad of crop.

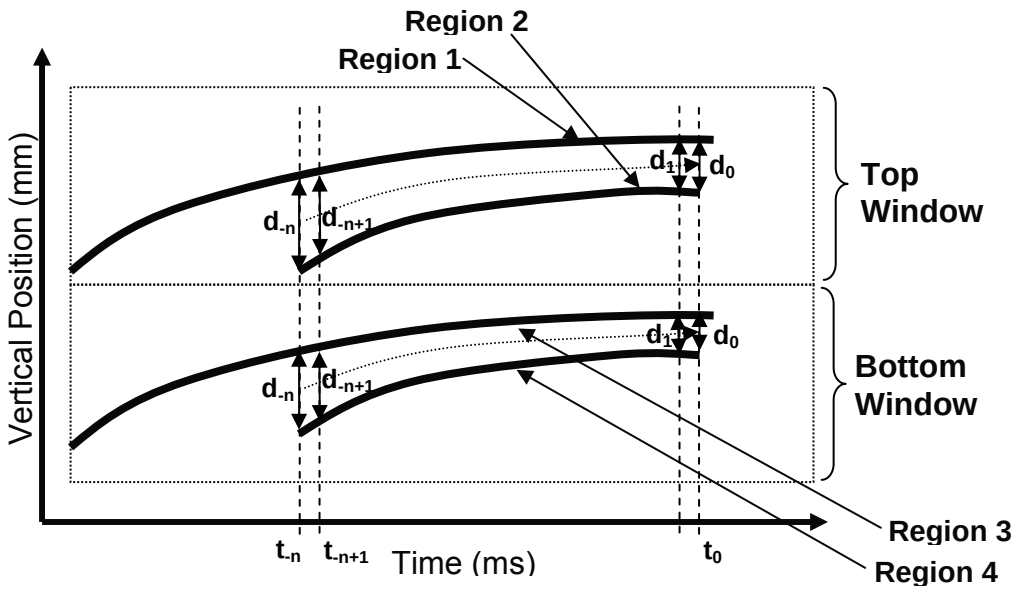

Figure 5.3 Theoretical example of flow from the precompression room to the compression chamber. Regions 1 and 2 illustrate the top and bottom particles tracked in the top viewing window. Regions 3 and 4 illustrate the top and bottom particles tracked in the bottom viewing window. The vertical distance between the particles at time $t_0, t_1, \ldots t_{-n+1}, t_{-n}$ are represented as $d_0, d_1, \ldots d_{-n+1}, d_{-n}$, respectively.

Referring to Figure 5.3, Region 1 and 2 represent the particles tracked in the top viewing window and Regions 3 and 4 represent the particles tracked in the bottom viewing window. The vertical distance between the particles in each window are represented by the variable d. The distances (d) between these particles were calculated at time t which corresponded to the frame in which the particles were recorded. The crop strain was calculated as follows for both top and bottom viewing windows:

$$\delta_i = \frac{d_{-n} - d_{-n+i}}{d_{-n}}, \tag{5.4}$$

where:

δ_i = crop strain calculated at i = 0,1, 2 … n-1,

d_{-n} = initial distance between particles (t_{-n}) and

d_{-n+i} = distance between top and bottom particles at time t_{-n+i}.

The distance d_{-n} was identified as the initial distance between the two particles once both particles were visible within the viewing window. All crop strain calculations were based from this initial distance. By establishing the strain calculation from this initial distance, this identified if the crop was moving vertically closer together or further apart throughout the course of its trajectory.

From the set of calculated strain values for one ejected wad of crop, average strain values were calculated for both top and bottom viewing windows as follows:

$$\delta_{Average} = \frac{\delta_1 + \delta_2 + ... + \delta_n}{n}, \tag{5.5}$$

where,

$\delta_{Average}$ = average strain value and

n = number of recorded strain measurements.

Peak strain values were identified as the absolute maximum or absolute minimum strain value found within the data set from each of the viewing windows.

The average and peak values for all measured wads of crop are listed in tabular form found in Appendix D.

5.2. Pressure Analysis

The pressure data required numerous steps to organize and analyze. This section outlines the procedure followed to analyze the raw data recorded during field experiments. The objectives for analyzing the pressure data were to compare the significance of the mean top and mean bottom plunger pressures, to develop profiles for plunger pressures (top and bottom) verses plunger displacement and to develop a model to examine the differences in measured bale weights (F_{Top} - F_{Bottom}).

The data collected were recorded using two logging sources; data logger and CAN logger. Due to the substantial amount of data contained in each logger file, macros were written in a spreadsheet to standardize the procedure used and minimize the effort required to work through each repetition. Rather than discussing each macro in detail, the intent of this section is to clarify the general procedure, concepts and assumptions used. For detailed explanations of each step and an example of the of the macros' operation, refer to North American macro file and sample data on the accompanying CD (see Appendix E). The macro file and sample data are also listed for European conditions although detailed descriptions of each step are not specified because both methods were analogous.

The macros represented an integral part of the analysis procedure although the final steps were performed using SAS (SAS Institute, Cary, NC) system. In the SAS environment, mean plunger pressures were compared and steps were carried out to develop a regression model. The procedures used in SAS are discussed in the closing stages of this section.

For discussion purposes, the data logger will be referred to as DAQ (data acquisition) and CAN logger will simply be referred to as CAN.

5.2.1. Timing CAN with DAQ

To utilize the recorded data, the CAN and DAQ files needed to be combined into one usable form. The DAQ was sampled at 250 S/s and required the CAN data to be aligned with the DAQ measurements at this same sampling rate. For the CAN data measured in Europe, the CAN logger recorded at the same sampling rate of 250 S/s and the two files only needed to be aligned at a point in time. However, for field tests in North America, the CAN logger only recorded when the bus changed state (event triggered) therefore, the CAN data needed to be timed to a sampling rate of 250 S/s as well as aligned with the DAQ data. The following describes how files for each of the European and North American circumstances were combined.

For the European data, although both loggers sampled at the same rate, the CAN data still required alignment so the measured events emerged at the same time. Before the CAN data could be aligned, the recorded CAN signals were translated from hex values to decimal values and then converted into engineering units using a mathematical expression provided by the manufacturer. The two logging sources were then aligned based on visual inspection of the sensor outputs. At the beginning of the tests, the pressure sensors mounted on the plunger would pulsate with consistent amplitude and then spike as shown in Figure 5.4 when the first wad of the run was ejected from the precompression room. Hence, the first recorded stuffer engagement from the CAN was timed with the first spike from the pressure sensors measured on the DAQ. For conversion of the CAN data into engineering units and timing with DAQ, these steps were manually completed without using macros.

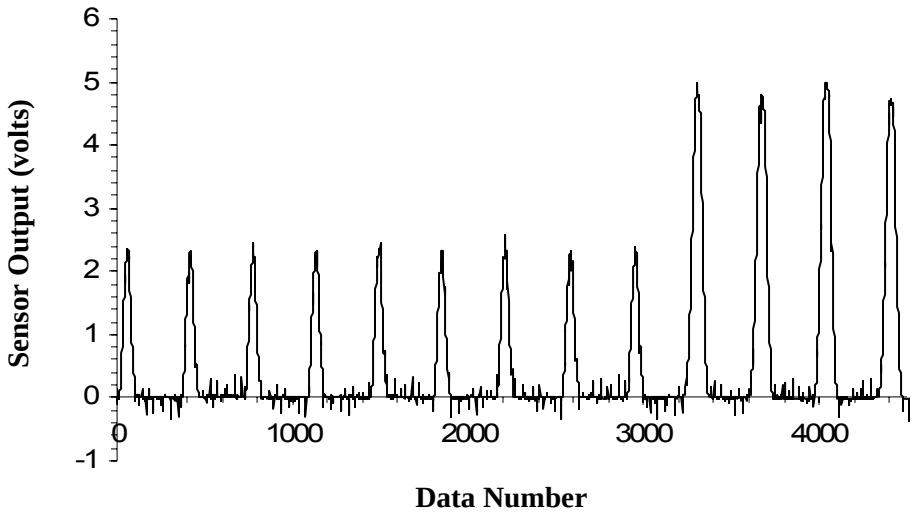

Figure 5.4: Pressure rise due to crop entering the bale chamber (data number ≈ 3325)

For the field tests in North America, due to availability of equipment, different hardware and software were used to record the CAN signals. This required the CAN data to be timed and aligned with the DAQ data. As with the European data, the recorded CAN signals were stored in the form of hex values and required the same conversion method to engineering units. For each recorded measurement on the CAN logger, the time of the sample was recorded in the form of a timestamp. Based on the associated timestamp, the CAN data were timed to the same sampling rate as the DAQ (250 S/s) by knowing that the state of each signal would not change until the next event occurred on the bus. For alignment of the CAN data with DAQ data, an additional sensor on the DAQ was logged to assist in the alignment process. A magnetic reed switch was installed and output was recorded on the DAQ to duplicate the similar reading of the stuffer engagement recorded by the CAN logger. The readings taken from the magnetic reed switch were noisy, but adequate to ensure proper alignment of CAN signals with DAQ. Figure 5.5 illustrates both recorded stuffer engagement from the CAN and stuffer engagement recorded by DAQ. Note the similarities of the two signals used for alignment.

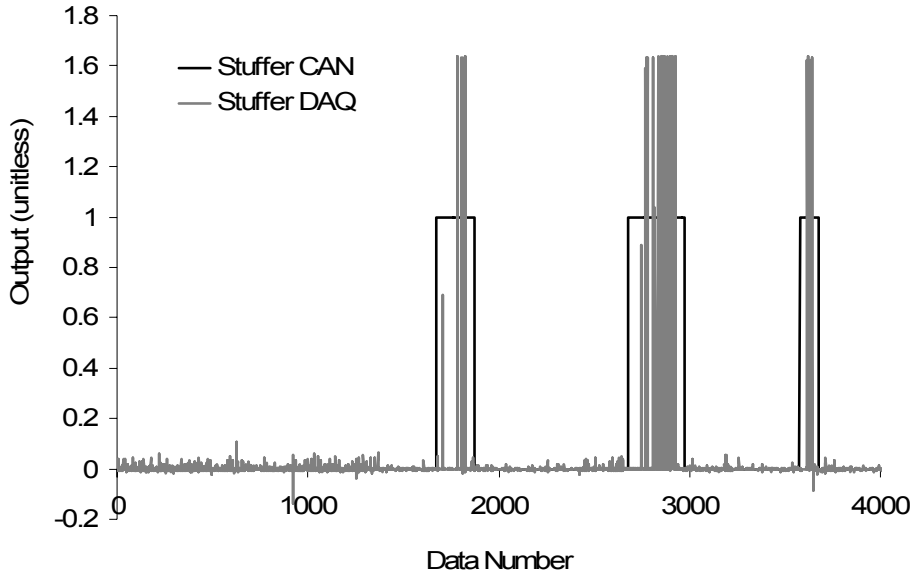

Figure 5.5: Stuffer engagement as measured by CAN and DAQ (North American Data)

The above alignment methods (both North American and European) were used to determine the approximate alignment position of the CAN data with the DAQ data. Knowing which stuffer engagement corresponded to a particular plunger cycle, the data were merged by recognizing that the stuffer was synchronized to reset at approximately the most forward position of the plunger stroke.

5.2.2. Locating Bounds

Once all the data were combined into one file, the bounds (starting and ending points) for the analysis were established and the bound data were isolated from all the recorded data to accommodate continued analysis procedures. The bound data represented the measured parameters which made up the formed bale. The starting point for the bounds was defined as the midpoint of the first knotter signal. The midpoint of the knotter signal would signify the approximate moment when a knot was tied to complete the previously formed bale and the tying of a second knot for the start of a new bale (beginning of the run). The endpoint for the bounds was defined as the center of the second knotter signal plus the time to reach the most forward stroke of the current plunger cycle. The reason the bounds end at the most forward stroke of the current plunger cycle and not ending at the center of the second knotter cycle was because the

center of the second knotter cycle would occur when the plunger was near its most rearward position. To record the entire pressure profile during the compression of the last wad of crop (including the rebound effect), the data were recorded until the plunger reached its most forward position. Figure 5.6 graphically illustrates both CAN and DAQ data. From Figure 5.6, the dashed box represents the approximate data defined as the bounds for one data set or the data collected for the formation of one bale.

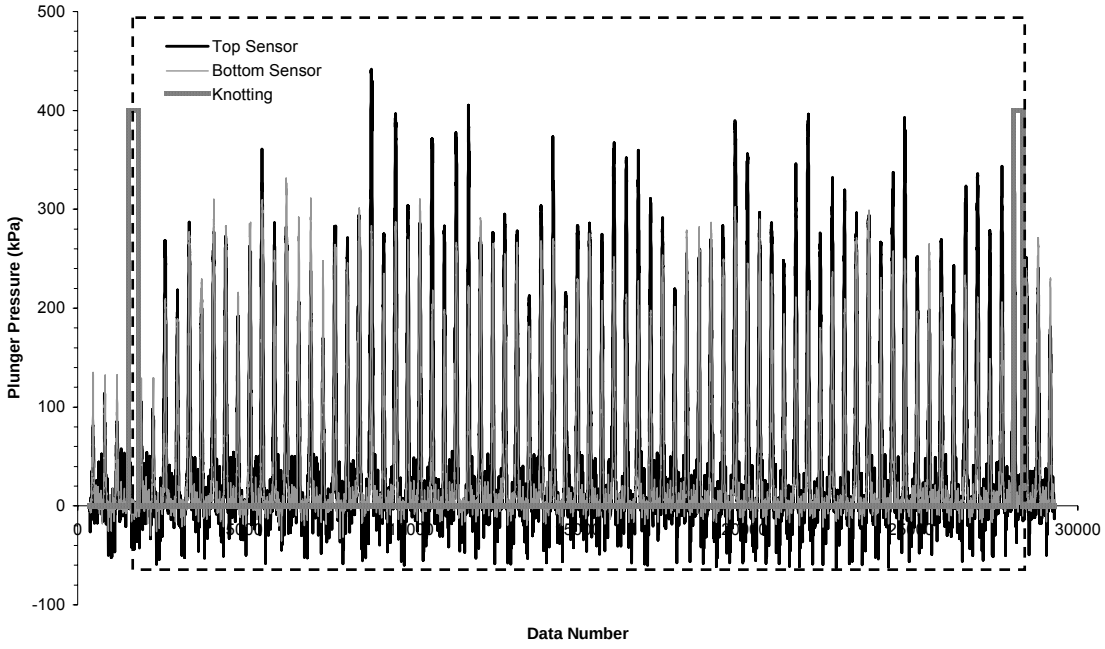

Figure 5.6: Combined CAN and DAQ data illustrating approximate bounds

5.2.3. Preparing to Segregate Crop Pressure

Preparing to segregate the data into crop pressures during formation of a flake was a fundamental step because during this stage critical processes were defined. These critical processes provided the bases for the results. This section outlines the logic, assumptions and processes used to structure the data for further analysis.

The raw logger data contained continuous streams of voltage output relative to the pressure acting on the sensors. This continuous stream of data represented the pressure acting on the plunger for the formation of one bale. To distinguish the pressure output for the duration of one plunger stroke, the data needed to be segregated into individual plunger strokes, timed with

corresponding plunger strokes and the pressure output evaluated at each plunger position. The following describes the preparation for these steps.

For the North American data, the first procedure was to apply a filter to both the bottom left and bottom center sensors to remove unwanted noise. For the bottom left sensor, a 15 point moving average was used to smooth the data set and, for the bottom center sensor, a 9 point moving average was used. All other sensors did not require filtering as the clarity of the signal did not warrant a filter to be applied. The number of points used for the moving average was dependent on the cyclic trends occurring within the unwanted noise.

With the unwanted noise filtered, each plunger stroke was reset to zero to account for drift of the amplifiers. In the vicinity of the most forward plunger position, the plunger was not in contact with any crop, hence, the applied pressure acting on the sensors should be zero. An average was taken for 50 points before and 50 points after the most forward stroke (100 points total) and the calculated average value was subtracted from each data point over a complete plunger cycle. The calculation for zeroing the amplifiers was conducted on each sensor for every plunger stroke.

Several processes were applied to the data and were referred to as logistical indicators, maximum counts, stuffer ratio and cycle time statistics. These processes were necessary procedures before the pressure data were segregated. Each process provided information to indicate the location for separation of the data or quality assurance information to verify each method was correct. The defined regions of data for export were; the pressure profile over a complete plunger stroke, and only those plunger strokes which compressed a wad of crop into a flake were analyzed. Logical indicators were used to highlight the beginning and end of each plunger stroke that compressed a wad of crop. Using these indicators, the plunger stroke which took the longest time to cycle was determined and stored as the maximum count. This maximum count was used to align the data when separating into individual plunger strokes and is further discussed in the next section. The stuffer ratio and statistics of the percent load, wall pressure and plunger cycle time were determined for the formed bale defined by the bounds. The stuffer ratio was calculated as the total number of plunger strokes divided by the total

number of flakes in the bale. The values for percent load and wall pressures were averaged over the course of the formed bale (bounds). Standard deviation, variance, maximum/minimum values and 95% confidence intervals were also determined for the percent load, wall pressures and the plunger cycle times.

The plunger cycle time was determined for every plunger cycle and then only the plunger cycles which formed a flake. The purpose for comparing the duration of the plunger cycles were to establish a sense for the amount of variability there was between plunger strokes. Generally, the cycle times were within a range of 10 ms.

5.2.4. Segregating Crop Pressures

For every wad ejected from the precompression room, the pressure data associated with the compression of the wad of crop throughout one complete plunger cycle (furthest forward stroke to furthest forward stroke) were segregated into individual plunger strokes. The data were aligned at the end of the compression stroke (furthest rearward stroke) by assuming the median data at the time to complete one plunger cycle, was the end of the compression. Once aligned, the voltage output from the pressure sensors were translated into pressure (kPa) utilizing the calibration equations determined in Section 4.3. The resulting pressure profiles were then averaged over every wad of crop to determine a resulting average pressure profile representative of the bale produced. Peak plunger pressures were determined for every wad of crop compressed and a single average peak pressure was determined from the average pressure profile. The set of peak plunger pressures were used for mean comparison between sensors and the single average pressures were used for model development.

5.2.5. Preparing Analysis File

Up until this point, the analysis has only been concerned with setting up results from individual formed bales. This stage of the analysis involved getting the results from all the formed bales into one new file. The results stored in the new file were used to compare peak plunger pressures, to create pressure graphs for top and bottom sensors and to develop a model to investigate differences in top and bottom bale weights.

For mean comparisons and model development, further analyses were conducted using SAS. Importing data into SAS required the data to be in a specified format and creation of the new analysis file was approached following the convention required. The resulting data from each formed bale were exported into the analysis file separating into three components of the analysis (model, graphs and means). During transfer of data into the model development spreadsheet, the bale weights, flake setting and named bale number were manually entered into the file.

5.2.6. Mean Comparisons of Peak Plunger Pressures

Plunger pressures were used to evaluate the integrity of repetitions, and plunger pressures were also used to identify if there were significant differences between the top and bottom plunger pressures. Peak plunger pressures were compared using the Duncan Multiple Range Test (DMRT) and analyses were performed using SAS software. Sample SAS codes and output for mean comparisons are illustrated in Appendix C.

5.2.7. Pressure Profiles Top and Bottom

Pressure profiles for each of the seven settings were created. The pressure data for each run were manually aligned with other runs at the median data point, which was assumed to be the furthest rearward portion of the stroke. The data for each run were again averaged, this time over each produced bale (rather than each compressed wad of crop) and the standard deviation was also determined indicating the average pressure fluctuation amongst the bales.

The pressure data were plotted versus plunger position and required a conversion from time to displacement. It was assumed the plunger-crank was rotating at a constant rate and the total number of data points could be divided by 360° to determine the degree increment for each point. The degree value was converted into plunger position using Equation A.20 derived in Appendix A.

5.2.8. Model Development

Mason et al. (2003) presents a comprehensive regression analysis which uses the acronym PISEAS (plan, investigate, specify, estimate, assess and select) as a guideline for model development. This PISEAS approach was followed to develop a regression model and forms

the layout for this section. Each phase was tailored to fit the requirements of the objectives and this section briefly describes the procedures and concepts used to create the regression model. Further details and methods explained here can be found in Appendix E.

The first phase of the PISEAS approach was to plan the data collection effort. This phase occurred before the data were collected by developing a sampling technique which provided representative data of the system under inspection. During field experiments, the settings used were randomly selected to avoid unwanted bias, and environmental conditions were monitored for possible changes.

From the collected data, the next procedure was to investigate for obvious errors and visually observe the trends that had occurred. The measured data were plotted against data number and against the difference in measured bale weights (dependent variable) for every predictor variable used in the model. When plotting the measured data against the data number, the plots were visually scanned for outliers to identify possible non-random patterns occurring within the data. There were no extreme outliers noticed and outliers were further investigated at the Assess stage of the PISEAS model-development technique. All plots were well distributed and there was no indication of non-random patterns (such as, abrupt shifts or cyclic trends) occurring within the data.

Plotting the response and predictor variables was performed to help illustrate the relationship between the two variables. Such plots may illustrate nonlinear trends occurring and thus indicate one or more variables must be re-expressed prior to creating the model. All data were well distributed and there was no indication the data needed to be re-expressed.

Simple summary statistics such as the mean, standard deviation, maximum and minimum values were determined for each variable to help acquaint one with the data. The summary statistics were used to review plots of each variable and to re-examine possible outliers.

The specify stage of the PISEAS technique involved specifying the form of regression model to use. One must not only consider the functional form but also interaction terms, polynomial terms and nonlinear functions of the predictor variables to be included in the model. Specifying

the form of the regression model also relies heavily on one's understanding of the process being studied. Knowledge of the process is important to decide which variable to include in the experiment and hence, the model, but also when questioning the functional form of the model.

From inspection of the response verses the predictor variables, all variables were assumed to be linear functions of the dependent variable. There was no indication based on the plots that the variables needed to be re-specified in a non-linear form.

No attempt was made to re-specify the difference in plunger pressures to a theoretical base. The reason was because theoretical models rely on knowledge of the modulus of elasticity for the crop material. In practice, determining the modulus of elasticity is difficult because this value is continually changing due to environmental conditions. For this experiment, difference in plunger pressures was assumed to be linear functions of the dependent variable.

Interaction effects of two variables were also made available when developing the model. The interaction effects were used because of particular variables' dependence on other variables. One example was the flake setting and number of flakes as the flake setting is directly related to the number of flakes. For an increase in flake size, the number of flakes will decrease and for a decreased flake size, the number of flakes will increase.

The next stage in the PISEAS approach involved estimating the parameters in the regression model as usually conducted using computer software. Before the model parameters were estimated, one-variable models were created to analyze which variables had the greatest association with the dependent variable. Regression models of one-variable and the resulting R^2 values were ranked according to the highest R^2. Similarly, one-variable and interaction models were created comparing the interaction effects as well as the simple effects. Likewise, the results were ranked based on the corresponding R^2 value. Sample SAS code and output for stepwise regression can be found in Appendix C. For complete source code and output refer to the electronic files found on the accompanying CD (see Appendix E).

Before the final model was developed, the data were split into training and test sets. Out of the 29 bales used in this study, 9 of the bales were selected as a test set and 20 bales were used to

train the model. The test set was randomly selected although, of the 9 bales, it was ensured that equal numbers were selected from each setting to avoid biasing selection from one particular setting. The bale numbers selected were 4, 6, 9, 11, 16, 19, 20, 28 and 29 (see Appendix B).

A forward selection stepwise regression approach was used to develop a model because there was a large number of predictor variables which could be included in a reduced model. The forward selection method finds the best predictor variables by adding one variable at a time. The selection method starts a model of one variable, finding the variable which produces the best fit, based on reducing the error sum of squares. Once the selection of the best one-variable model is satisfied, the procedure is incremented to a model of two variables. This process continues until the addition of a predictor does not materialize further significance or all parameters are used in the model.

The stepwise regression approach was employed on the basis of reducing the error sum of squares. One concern for using the stepwise regression approach was the significance level to use when detecting candidate predictor variables. Because the predictor variables were determined from the error rates, care was taken in selection of the type of error rate used to avoid excluding noteworthy predictors. A recommended practice to protect against losing noteworthy predictors was to use a much larger significance level, such as $\alpha = 0.25$, when utilizing the stepwise method (Mason et al., 2003).

To create a credible model, the assumption was made that a minimum number of 5-10 data points were required for the inclusion of every predictor variable. Hence, for a training set of 20 data points, the maximum number of possible predictor variables included in the final model would be no greater than 4. The models were developed using SAS software and sample code and output can be found in Appendix C.

Once the models were developed, the next stage involves assessing the adequacy of the models. There were two main topics of concern; outlier detection and evaluating the adequacy of model assumptions. The intent here is to briefly outline each topic. For further information, the author references Mason et al. (2003).

Outliers were detected using Grubbs test. The procedure involved calculating critical values for the suspect outliers (largest and smallest values within each data set) and comparing the calculated value to corresponding critical values. All comparisons were based on a 5% significance level.

Another assumption used in regression analysis was that the regression model has normally distributed errors. The Shapiro-Wilk test was used to determine if the model had normally distributed errors. As with outlier detection, all comparisons were based on a 5% significance level.

For this study, the variables were assumed to be linear. To examine this assumption, a simple regression fit was determined between the dependent variable (difference in weight) and each of the predictor variables. From the regression equation, the residuals from each predictor variable were summed and plotted against the run numbers. Residuals was calculated as the

$$\text{Residual} = \Sigma(\text{measured value} - \text{calculated model value})^2 \qquad (5.6)$$

The two variables with the highest sum of residual were the percent load and the number of flakes. From inspection of the residual plots, there were no apparent trends indicating that either variable required re-specification. Also, modifying variables to nonlinear or power form would greatly increase the complexity of the model. For these reasons, the assumption of linear predictor variables was appropriate for the requirements of this study.

To select the best model, each model was compared to the test set and the model with the lowest residual was selected as the best generalized model. Section 6.5 discusses the results for the developed model.

6. RESULTS AND DISCUSSION

6.1. Video Results – Filming From Side

The resulting projectile plots are illustrated in Figure 6.1 and Figure 6.2 for Regions 1-2 and Regions 3-4, respectively. The fitted trend lines which were defined in Section 5.1.4 are also shown on both Figure 6.1 and Figure 6.2. The trend line for the projectile motion take the form of a second order polynomial as shown in the following equation:

$$y_v = at^2 + bt + c \text{ (mm)} \tag{6.1}$$

where:

y_v = vertical displacement (mm),

t = time (ms) and

a, b and c = experimental coefficients

The vertical velocity ($v_{vertical}$) and vertical acceleration ($a_{vertical}$) were the first and second derivatives of Equation 6.1. The vertical velocity was calculated as

$$v_{vertical} = 2at + b \text{ (m/s).} \tag{6.2}$$

and the vertical acceleration was calculated as:

$$a_{vertical} = \frac{\partial^2 y_v}{\partial t^2} = 2x10^3 a \text{ (m/s}^2\text{)} \tag{6.3}$$

Solutions to the above coefficients (a, b and c) were determined in Section 5.1.4 and are listed in Table 6.1 for each region. The assumption was made that the velocity of the crop was zero at time t = 0, therefore the b term was zero for all cases and is not listed in Table 6.1.

Table 6.1: Coefficients for Equations 6.1-6.3 for Regions 1-4

	a	c
Region 1	-7.38×10^{-3}	616
Region 2	-10.6×10^{-3}	525
Region 3	-12.9×10^{-3}	167
Region 4	-18.7×10^{-3}	63.2

*b = 0

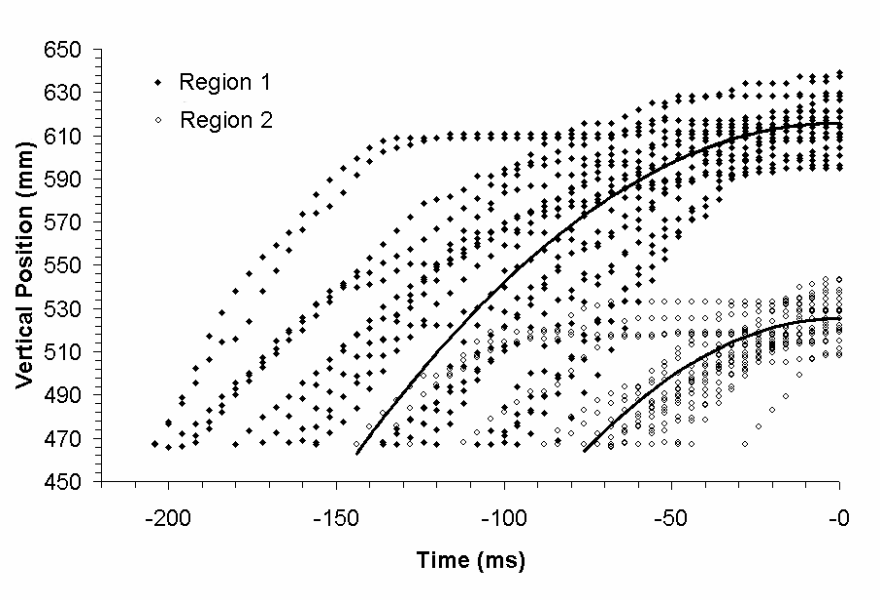

Figure 6.1: Resulting vertical displacement for crop trajectories in Regions 1 and 2

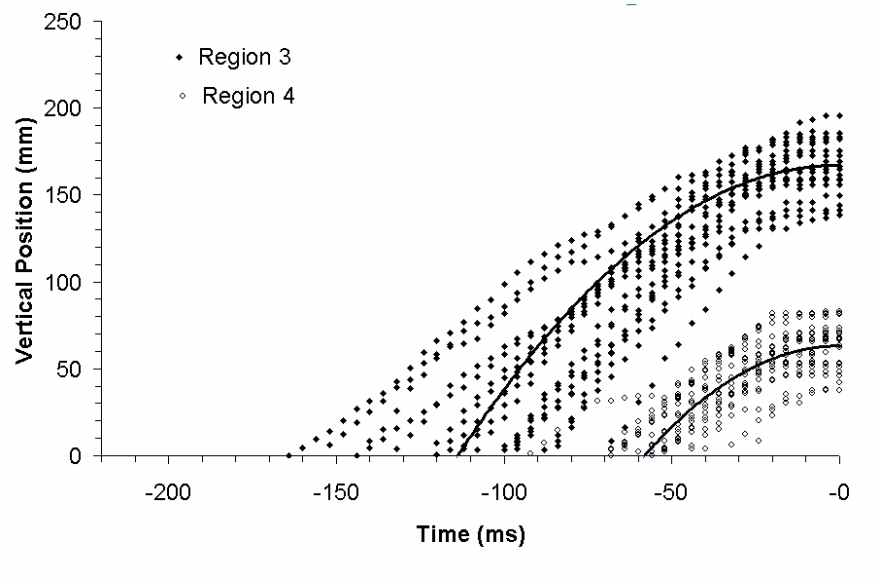

Figure 6.2: Resulting vertical displacement for crop trajectories in Regions 3 and 4

The crop's trajectory followed a parabolic curve similar to projectile motion. The fit of the trends were adequate in terms of requirements for the objectives. However, from visual inspection, they may appear to be more linear before contact with the ceiling of the bale chamber when they abruptly cease movement in the vertical direction. Deceleration for the fitted trend lines ranged anywhere from approximately 15 m/s^2 for Region 1, to 37 m/s^2 for Region 2.

The strain was described two ways; average strain and peak strain. The average strain measured from the side of the baler was 12.8% for the top and the average strain for the bottom was 2.1%. The resulting peak strain was 22.6% for the top and 8.7% for the bottom. Assuming equal initial density, this implied there was a higher density in the top compared to the bottom upon compression of the wad of crop by the plunger. Figure 6.3 illustrates the results for both average and peak strain values measured from the side of the baler.

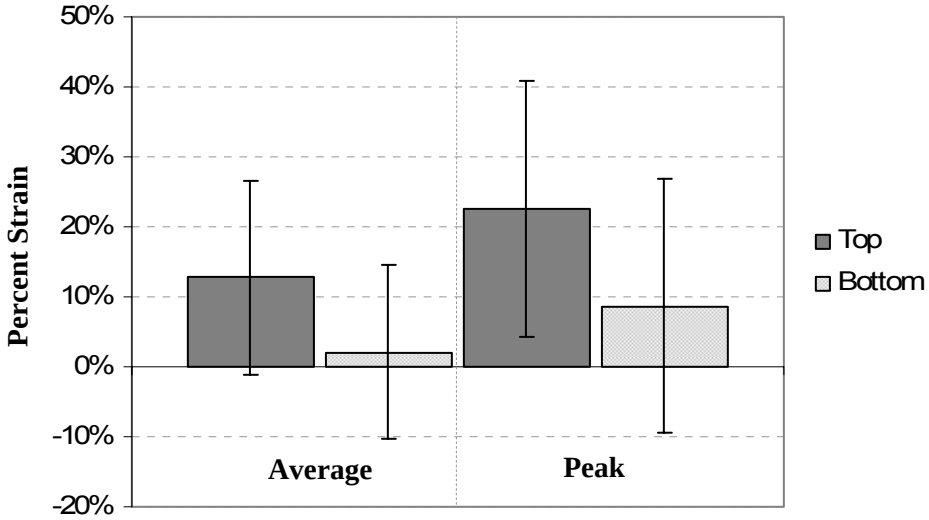

Figure 6.3: Resultant strain values from side view. Error bars represent standard deviation.

As shown for both the crop trajectory of Figure 6.1-6.2 and the strain values illustrated in Figure 6.3, there was variability among the data. The crop trajectory could have varied for several reasons. If the precompression room was filled with more crop material on one side compared to the other, the initial wad of crop would be inconsistent from side to side in relation to density

and affect the repeatability of each sample. During the analysis, the assumption was made that the wad of crop inside the precompression room was of uniform density and thickness before being ejected. If this assumption was not valid, the density variation may be related to the initial wad of crop in the precompression room. Varying moisture content due to humidity, time of day or location within the windrow could also affect the material properties of the crop causing the material to behave differently upon ejection from the precompression room. Similarly, contaminants (such as weeds) or length and orientation of the crop could affect the flow pattern causing the results to vary.

It is probable the crop motion may have varied from one wad of crop to the next although, the methodology used should also be examined. Two main concerns to take into account were; tracking the crop's motion and locating the plunger's center position.

Acquiring a representative measurement of the crop trajectory required correctly targeting and tracking the crop's motion. The difficulty in tracking the crop arose due to several reasons:

- Due to the turbulent motion of the crop, targeted points would be lost while tracing the motion.
- Low resolution or focus of the camera affected the quality at which particles could be identified.
- Improper alignment of lighting occasionally affected locating particles due to problems with glare.
- Crop adhering to the glass caused the viewed surface of motion to be different from the core of the crop's motion.

Another difficulty was accurately determining when the plunger's face was centered in the viewing windows due to problems with crop wrapping around the plunger's edges, obscuring a distinct view of the plunger's face. Aligning the plunger's position in the center of the viewing windows played a crucial role in establishing the start of the data collection process. Uncertainty about the plunger position affected the displacement curves in relation to time.

6.2. Comparing Peak Plunger Pressures

The plunger pressures were compared for two main purposes; 1) to identify if repetitions of similar settings were of equal measure and 2) to identify if top and bottom compression pressures were of equal measure. Calculations were conducted using DMRT (see Section 5.2.6) method to test the significance of the peak plunger pressures.

Comparisons between repetitions were conducted by comparing the means of peak pressures for each sensor. Based on the results shown in Appendix D, the observed trend was that the repetitions of similar settings were not always equal based on a 5% significance level. However, variations in repetitions could be accounted for by several possibilities; the changes in crop moisture content, the resulting stuffer ratios differed, the initial mass of crop delivered fluctuated, the introduction of foreign material, and the orientation and length of crop varied.

The focus for this research has been to compare top versus bottom flake densities prior to being pushed through the bale chamber. The effects of the bale chamber walls could be conceptualized similar to pushing steel through a die. The bends in the bale chamber wall form the bale into its final shape. Differences between top and bottom plunger pressures would suggest the top and bottom flake densities were dissimilar prior to going through the bale chamber walls. Means of peak plunger pressures were compared between sensor locations for each setting and the results are listed in Table 6.2.

The results for comparison of means between locations indicate the means were different between top and bottom sensor location based on a 5% significance level with the exception of setting 4, where the means for top and bottom peak pressures were equal. The comparison was also conducted for side to center location by comparing the peak pressures between the bottom left and bottom center sensors of setting 1. The results revealed the means of peak pressures were different from the bottom left to bottom center location which would suggest there was a density gradient from left to center. The reason there was a difference in density could be related to effect of the side augers pushing more material towards the left and right chamber walls. Wall friction could also have a significant role causing a decreasing pressure gradient

towards the center. Bends in the bale chamber wall would also increase the force required to push the wad of crop through the bale chamber at the outer most locations.

Table 6.2: Comparisons of Peak Pressures for Top and Bottom Locations

Setting	Flake Setting	Wall Pressure	Location*	Mean (kPa)	Standard Deviation (kPa)	Duncan Grouping
1**	Medium	80% Constant Density	TL	494	106	A
			BL	403	71	B
			BC	276	68	C
2	Thin	11 MPa	TC	300	52	A
			BC	282	37	B
3	Medium	11 MPa	TC	369	91	A
			BC	322	79	B
4	Thick	11 MPa	BC	318	57	A
			TC	318	77	A
5	Thin	7 MPa	TC	240	50	A
			BC	217	33	B
6	Medium	7 MPa	TC	236	44	A
			BC	186	31	B
7	Thick	7 MPa	TC	218	50	A
			BC	188	27	B

*TL = Top Left, BL = Bottom Left, TC = Top Center and BC = Bottom Center (refer to Figure 6.4)

**North American Data

The plunger pressures suggested the density was higher or lower at top versus bottom location (or side verses center) upon compression into a flake. Figure 6.4 illustrates the sensor locations for test apparatuses used in North America.

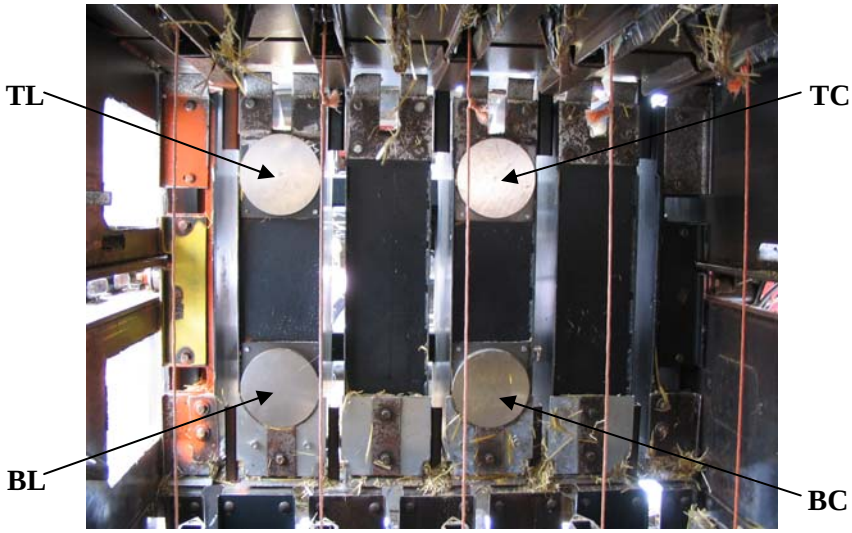

Figure 6.4: Identification of sensor locations, top left (TL), bottom left (BL), top center (TC) and bottom center (BC). Test apparatus for North American configuration shown.

The top center sensor in the North American data (setting 1) was omitted from comparison of means due to faulty instrumentation. Although the loss of the sensor was unfortunate, the sensors located on the left of the machine were used to account for this loss. Hence, for the North American data (setting 1) the comparison of pressures between top and bottom were compared on the left of the machine rather than the center. Implications of sensor location and design are further discussed in Sections 6.4 and 6.5.

6.3. Plunger Pressure Profiles

The pressure profiles for each setting were used to help describe the compression process and compare compression between top and bottom locations. The resulting pressure curves for each setting are illustrated in Figures D.1 to D.8 (see Appendix D). From the pressure profiles, there are several recognizable features; the location where the plunger made initial contact with the crop, the peak pressures before over-coming static friction then shifting the bale in the chamber, the rebound effect occurring on the return stroke of the plunger, and the variability of the average plunger pressure throughout one plunger cycle.

The initial contact with the crop was identified as the point where the pressure initially began to rise. The pressure rise generally occurred earlier at the top location compared to the bottom. The increase in pressure rise could possibly be caused by the geometry of the bale chamber. The bale chamber has bends at both top and side walls and no bend along the bale chamber floor. The pressure would increase earlier at the top due to the funnel effect and require more pressure to push the wad of crop due to the increased resistance.

The peak pressures indicated when the crop had been compressed to its fullest and overcomes static friction to shift the bale to the rear of the machine. The density of the flake immediately prior to being pushed through the bale chamber walls was of importance to determine if the density was affected by the chamber walls or the precompression room. The peak pressures from the pressure profiles and resulting percent difference in bale weights are illustrated in Table 6.3. Sample calculations for determining percent difference in bale weight are provided in Appendix A.

Table 6.3: Peak Pressures and Percent Difference in Final Bale Weights

Setting	Flake	Wall Pressure	Location**	Peak Pressure (kPa)	Percent Difference Bale Weights*
1	Medium	80% Constant Density	TL	482	-0.14%
			BL	383	
			BC	270	
2	Thin	11 MPa	TC	291	-1.94
			BC	274	
3	Medium	11 MPa	TC	356	3.14%
			BC	313	
4	Thick	11 MPa	BC	307	3.31%
			TC	312	
5	Thin	7 MPa	TC	220	-1.39
			BC	214	
6	Medium	7 MPa	TC	215	3.55%
			BC	182	
7	Thick	7 MPa	TC	196	3.54%
			BC	185	

*Negative indicates bottom was heavier than top

** TL = Top Left, BL = Bottom Left, TC = Top Center and BC = Bottom Center (refer to Figure 6.4)

The primary advantage of the pressure profiles was to provide a qualitative understanding of the compression process and only speculations can be made about the distinct cause of bale density differences. Through visual inspection, there appears to be a relationship between the flake setting and final difference in bale weights. As the flake setting is increased (from thin to thick), it appears the bale becomes heavy towards the top. There does not appear to be as firm of a relationship between difference in peak pressures and difference in bale weights. One speculation was that both the precompression room and the bale chamber would affect the bale density differences, although the flake setting compared to the precompression room would have the greatest effect.

The peak pressures and rise in pressures would be dependent on previously formed flakes in the bale chamber. The pressure may increase sooner and peak higher at one location compared to the other if the previous flake was adversely positioned so the front of the flake was not equally parallel to the plunger's face (for example, crop falling from the top of the previously formed flake).

The pressure profiles for setting 1 were distinct from the other set of sensors. As illustrated in Figure D.2, the erratic signal from the top center sensor indicated the sensor was faulty and

therefore, the sensors on the left hand side of the baler were used. The comparison of peak pressure measurements in Section 6.3 identified there was a pressure gradient between the left and center of the plunger, therefore, the left sensors may not have been an ideal substitute for this study. The sensors used for setting 1 were also a slightly larger design and different signal conditioning was used compared to the other settings. Implications of different sensor design and signal conditioning could possibly result in a different sensitivity from the sensors used in settings 2-7. Variations in crop density across each sensors' surface could also have an effect on the measured output as the diaphragm design was not ideal for measuring a semi-solid such as straw.

6.4. Developed Model

The model was developed to further explain the factors affecting the difference in measured bale weights and describe how these factors were related. One of the initial stages of model development was to estimate the parameters which had the greatest association with the dependent variable (difference in bale weight). Regression models of single variables were created and the resulting R^2 was ranked. Table 6.4 illustrates the rank and corresponding R^2 for each single-variable model.

Table 6.4: Resulting R^2 for Models of Single Predictor Variable

Rank	Variable	SSE	R^2
1	Flake Setting	1850	0.314
2	Chamber Pressure	2378	0.117
3	Number of Flakes	2544	0.056
4	Stuffer Ratio	2602	0.034
5	Difference in Top/Bottom Plunger Pressures	2615	0.030
6	Percent Load	2676	0.007

Table 6.4 indicates the flake setting and chamber pressure, have the greatest effect on the difference in bale weights.

Similarly, one-variable and interaction models were created comparing the interaction effects as well as the simple effects. The results of each model are ranked based on the highest R^2 and results are shown in Table 6.5.

Table 6.5: Resulting R^2 for Models of Single Predictor Variables with Interactions

Rank	Variable	SSE	R^2
1	(Flake Setting)*(Number of Flakes)	1458	0.46
2	(Chamber Pressure)*(Flake Setting)	1657	0.39
3	Flake Setting	1850	0.31
4	(Chamber Pressure)*(Stuffer Ratio)	1982	0.26
5	(Percent Load)*(Flake Setting)	1983	0.26
6	(Stuffer Ratio)*(Flake Setting)	2187	0.19
7	Chamber Pressure	2378	0.12
8	(Chamber Pressure)*(Percent Load)	2451	0.09
9	Number of Flakes	2544	0.06
10	(Difference in Top/Bottom Plunger Pressures)*(Stuffer Ratio)	2580	0.04
11	Stuffer Ratio	2602	0.03
12	Difference in Top/Bottom Plunger Pressures	2615	0.03
13	(Difference in Top/Bottom Plunger Pressures)*(Percent Load)	2619	0.03
14	(Difference in Top/Bottom Plunger Pressures)*(Number of Flakes)	2630	0.02
15	(Stuffer Ratio)*(Number of Flakes)	2633	0.02
16	(Percent Load)*(Stuffer Ratio)	2642	0.02
17	(Difference in Top/Bottom Plunger Pressures)*(Flake Setting)	2655	0.02
18	(Percent Load)*(Number of Flakes)	2655	0.02
19	(Difference in Top/Bottom Plunger Pressures)*(Chamber Pressure)	2666	0.01
20	(Percent Load)	2676	0.01
21	(Chamber Pressure)*(Number of Flakes)	2683	0

The results indicate that the flake setting and number of flakes have the greatest affect on the difference in top and bottom bale weights. Although related, both flake setting and number of flakes were expected to appear in the final model as these variables have the greatest influence on the dependent variable. The next expected variable to appear in the final model (from inspection of both Table 6.4 and Table 6.5) would be the chamber pressure. Failure for these variables to appear in the final model would indicate an error in the development process.

The model was developed by using a stepwise regression approach and selection of the model was conducted by comparing the trained data to a test set. Development of the models was computed using SAS software and the resulting models are listed in Table 6.6.

Table 6.6: Developed Models using Stepwise Regression

Number of Variables	Predictor Variables	Estimate	Pr > F	R^2
1	Intercept	-9.888	0.018	0.47
	(Flake Setting)*(Number of Flakes)	0.095	0.001	
2	Intercept	5.542	0.605	0.54
	(Stuffer Ratio)*(Number of Flakes)	-0.297	0.136	
	(Flake Setting)*Number of Flakes)	0.121	0.001	
3	Intercept	9.796	0.362	0.60
	(Stuffer Ratio)*(Flake Setting)	-0.740	0.136	
	(Stuffer Ratio)*(Number of Flakes)	-0.389	0.059	
	(Flake Setting)*(Number of Flakes)	0.182	0.001	
4	Intercept	4.436	0.669	0.64
	(Chamber Pressure)*(Percent Load)	0.013	0.136	
	(Chamber Pressure)*(Flake Setting)	-0.543	0.078	
	(Stuffer Ratio)*(Number of Flakes)	-0.499	0.032	
	(Flake Setting)*(Number of Flakes)	0.305	0.009	

The models were assessed for the presence of outliers and the presence of normally distributed errors. The results indicated there were no outliers present and the assumption of normally distributed errors was valid. All calculations were based on a 5% significance level.

Model selection was conducted by comparing the developed models to the residual. Figure 6.5 illustrates the plot of residuals against the number of variables. Referring to Figure 6.5, the best generalized model appears to be either a single variable model or a 3 variable model. The 3-variable model was chosen as the best generalized model because only 1 variable is unlikely to describe the phenomena of difference in bale weights from a large square baler.

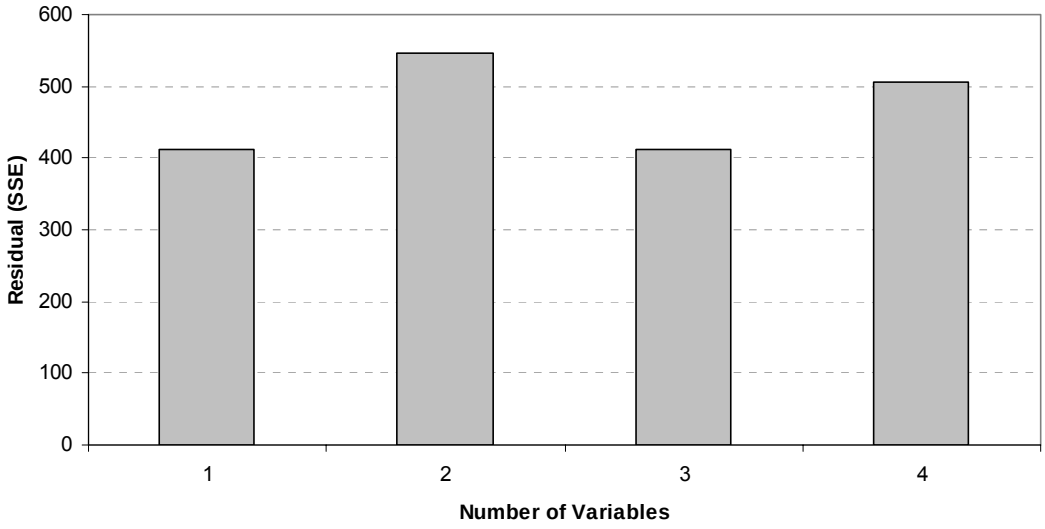

Figure 6.5: Model selection by residuals. As the number of variables was increased, the output of the model should become closer to the actual data and hence, the residual will decreased. If too many variables were added, the residual will increased because the output of the model becomes over-trained to the training set and the model loses its generalized form. The minimum values are shown to be that of 1 variable and 3 variables. The 3 variable model was chosen as the best generalized model because only 1 variable is unlikely to describe the phenomena of difference in bale weight in a large square baler.

Hence, the resulting regression model was,

$$\begin{aligned} DiffWT = &- 0.740 * StuffR * FlakeSet \\ &- 0.389 * StuffR * NumFlake + 0.182 * FlakeSet * NumFlake + 9.796 \end{aligned} \quad (6.4)$$

where:

DiffWT = measured difference between $F_{Top} - F_{Bottom}$ (see Section 4.4) (kg),

StuffR = resulting stuffer ratio (unit less),

FlakeSet = flake setting used (where thin = 1, medium = 4 and thick = 8), and

NumFlake = number of flakes in the bale (unit less).

The above equation and resulting single variable regression models show that the flake setting had the greatest effect on distribution of bale densities and the next highest relationship was the

stuffer ratio. The number of flakes identified the count of flakes within a bale but would also be directly related to the flake setting. Although bale chamber pressure does not appear in the final model, it did appear in the four-variable model which was rejected in Section 5.2.8.

The response of the three variable model (Equation 6.4) was compared to the test data and results are shown in Figure 6.6. The results show the test data were somewhat skewed to below the 1:1 trend line, indicating the model may need refinements. Such refinements may be including variables which were not identified in this study or redefining the structure of the model to non-linear form or a combination of both.

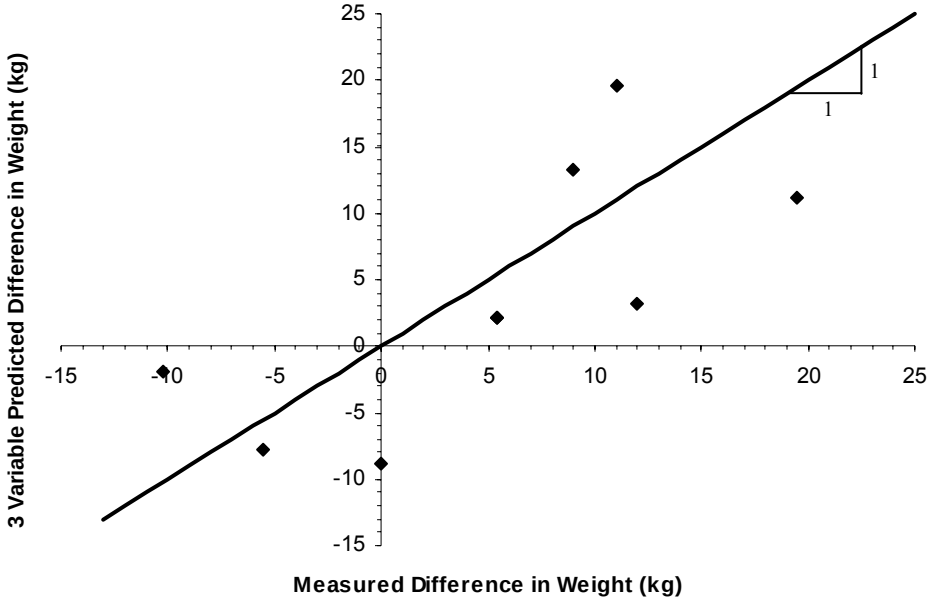

Figure 6.6: Comparison of model to test data. Predicted difference in measured bale weight for 3 variable model compared to measured test data. The test data appears to be somewhat skewed to below the 1:1 trendline which indicates the model may require refinement to include more variables, redefine to a non-linear form or both.

The resulting coefficient of determination (R^2) for the developed model was 59.9%. The resulting R^2 was low and could be due to the model lacking statistical power. One difficulty was collecting enough samples for efficient comparison of top and bottom bale densities. An entire bale needed to be formed and the data were averaged over the bale. Based on the number of variables which could affect top-to-bottom density differences, more samples would have

strengthened the analysis. However, due to time and cost limitations, the feasible number of samples was limited.

An advantage to developing a model to determine difference in bale weights would be to optimize the model and find solutions which minimize bale weight differences. The developed model can facilitate machine improvements and determine ideal settings to minimize bale density inconsistencies. For example, using an iterative technique to solve Equation 6.4, one solution to minimize differences in bale weights would be to use a flake setting of 1/10 and operate at a 1:1 stuffer ratio (solution was based on a bale of 40 flakes).

7. CONCLUSIONS

7.1. Video – Side Measurements

The video measurements were dependent on the initial wad of crop being ejected from the precompression room. Because the initial density of the crop within the precompression room was not known, the strain measurements were only relative to the initial crop density prior to ejecting from the precompression room. Assuming the crop prior to ejection was of uniform thickness and density may not be a valid assumption. This assumption needs to be validated before a confident statement can be made about the crop density during the ejection stage from the precompression room to the bale chamber.

The trend of the measured results indicates the strain was higher at the top half of the wad compared to the bottom during ejection into the bale chamber. If the assumption was valid that the crop leaving the precompression room was of uniform thickness and density, this would suggest the crop was becoming denser at the top compared to the bottom during this process.

The strain only suggests an increase in density during transport from the precompression room to the bale chamber as there are no scientific facts which support relating crop strain to density. Measuring the bale weights (top and bottom) after the bale has been pushed through the bale chamber walls would not necessarily verify this claim as the bale chamber walls could transform the bale (similar to pushing through a die) and have an effect on the density. Also, there are several difficulties using plunger pressures to measure density as discussed in section 7.3 and 7.4.

Determining the absolute density increase from measuring the crop strain is inconclusive. The projectile displacement, velocity and acceleration of the crop for four regions of the viewing windows were determined and results are shown in Equations 6.1-6.3.

7.2. Peak Plunger Pressures

The purpose of measuring peak plunger pressures was to identify the density before the crop was pushed through the bale chamber. The pressure output was found higher at the top sensor

compared to the bottom with the exception of setting 4 where there was no difference between top and bottom peak pressures based on a 5% significance level. Only for Setting 1 the comparison was made between side to center peak pressures and results showed the peak pressures were different. All mean hypothesis tests were performed using DMRT (Duncan Multiple Range Test) based on a 5% significance level.

The pressures were not converted into density because of the complexity establishing the pressure-density relationship. This relationship can change with material properties and baler geometry. The material properties can change by introduction of contaminants (such as weeds), change in moisture content or length and orientation of the crop. The baler geometry could affect the pressure density-relationship by processing the crop in a different method. For example, the baler could change the orientation and length of crop or the mechanisms used to hold the formed bale in the bale chamber could be different (ex. surface roughness, length and bend angle of bale chamber walls could affect the friction required to push the bale through the bale chamber).

Because of the difficulty in establishing an absolute pressure-density relationship, the results can only be compared relative to each sensor. Assuming the pressure difference between the sensors directly corresponds to density difference, the results would support there was a density difference from top to bottom for almost all settings at the stage of compression into a flake. Also, comparing the pressure difference to difference in bale weights, the bale chamber has a significant effect on altering the weight of the bale from top-to-bottom. The pressure was always higher at the top compared to the bottom whereas, the bale weights were sometimes higher in density at the bottom compared to the top.

7.3. Plunger Pressure Profiles

The graphs illustrating the pressure output versus the plunger's position assist only in qualitatively understanding the compression process for the particular baler used in this study and identifying the location of peak pressure rise. Generally, the pressure was found to rise earlier at the top sensor compared to the bottom and the resultant peak pressure would almost

always be higher at the top compared to the bottom. Resultant plunger pressures verses plunger positions are illustrated in Figure D.1 to Figure D.8.

7.4. Developed model

The developed model was shown in Equation 6.4. The model and the single variable regression analysis indicates the stuffer ratio, flake setting, chamber pressure and number of flakes were the most significant factors in the difference between measured top and bottom bale weights. The flake setting was found to be the most significant factor in effecting top and bottom bale weights.

An optimal solution was found to minimize difference in bales weights. The suggested method was to use a 1/10 flake setting and 1:1 stuffer ratio to minimize top/bottom density indifferences (based on a 40 flake bale).

8. FUTURE DEVELOPMENTS

Comparing the final measured bale weights from top to bottom, there was a maximum difference of approximately 5% in wheat straw. Ultimately, the end product (bale produced) must be of consistent density and ideally, the crop would be of consistent density during each process as well. If bale density variations are deemed to be inadequate and there are further studies to developing a more consistent product, this section presents possible recommendations for future reference.

8.1. Problem Crops

All experiments were conducted in wheat straw and may not have been the ideal material for identifying density differences. Using problem crops such as silage where density differences have been know to be more pronounced may help identify the underlying factors affecting bale density and would amplify the density differences.

8.2. Uniform Density Within the Precompression Room

Throughout this study, it was assumed the wad of crop was of consistent density upon leaving the precompression room. The validity of this assumption should be verified. A study needs to be conducted to determine the density variation within the precompression room immediately prior to the crop being ejected to the bale chamber. Variability of material density at the precompression room stage would likely be transferred to the final bale produced.

8.3. Robustness of Model for Differences in Bale Weights

The developed model for differences in bale weights aids in analyzing the baler from a global perspective and has value to forecast future studies. The model identified the flake setting, the stuffer ratio and the number of flakes as the most significant in affecting the consistency of the top and bottom bale densities although the model lacked statistical power. The low correlation of the model may not have enough significance to base sound judgments. Developing a more robust model would create increased confidence when addressing adjustments to specific components and assist in evaluation of future modifications.

Building a more robust model would involve increasing the number of samples and increasing the pool of variables to select a model which adequately describes the density differences. Selecting additional variables to measure would require an educated guess and a comprehensive understanding of the baler's operation.

Numerous variables could be included in a new model although the practicality of measuring them and the significance the variables will have on the model is debatable. Two possibilities may be to monitor the PTO speed and the amount of time the precompression room was full. The PTO is mechanically linked to the plunger and stuffer drive mechanism. The PTO speed may vary due to crop throughput and hence, affect the speed at which the crop is ejected from the precompression room. Also, the stuffer sensor located at the bottom of the precompression room was of consideration. The stuffer forks were mechanically linked and timed to the plunger cycle although the trip of the stuffer sensor was independent of the plunger. Depending on when the stuffer sensor was tripped, there was a delay before the stuffer forks were engaged and the precompression room was emptied. Depending on the duration of this delay, more crop could be pushed into the precompression room. Including the amount of time the stuffer sensor indicated full before being reset could possible account for some of the variability among the data.

The recommendation is to build a more robust model from a full season of data, encompassing all environmental conditions. The model would include variables listed in this study plus additional PTO speed and duration of time the precompression room indicated full.

8.4. Refining Projectile Motion Analysis

The projectile motion of the wads of crop were analyzed for only one flake setting, only in wheat straw and no modifications were made to the machine. The projectile motion (video) analyses combined with model development greatly exemplify the dynamics of the trajectory. However, adjustments of key parameters such as the stuffer fork speed or flake setting may increase the field of view towards tuning the machine for consistent bale output. However, if continued video analyses are used, modifications to the approach are recommended.

Filming from the side worked well although the plunger rails obscured the field of view and there was difficulty in tracking the crop. For continued analysis, it is recommended that tracer particles need to be introduced. Tracers must be selected or designed so they *specifically follow* the motion of the crop. Failing to do so could potentially result in an inconclusive study.

Filming from the rear was arguably more accurate than filming from the side and filming from the rear was able to capture the entire field of view. However, filming from the rear was time consuming and the injection of the light emitting diodes (LEDs) varied among the different material quantities in the precompression room. Automated injection of tracer particles and triggering both HSC (High Speed Camera) and DVC (Digital Video Camera) upon the trip of the stuffer sensing mechanism would enhance the performance of this experiment. Also, detection of the wad of crop reaching the top of the bale chamber was impossible without inspecting the vertical displacement versus time graphs. Inclusion of indicators to supply feedback once the wad of crop reaches the roof of the bale chamber or contact has occurred with the plunger would help standardized the trajectory measurements.

9. REFERENCES

Agriculture and Agri-Food Canada. 2006. *Canada's Forage Industry*, Suppliers & Products Fact Sheets. URL: http://atn-riae.agr.ca/supply/factsheets/3303_e.pdf.

Canadian Food Inspection Agency. 2005. *Livestock Feeds*. URL: http://www.inspection.gc.ca/english/anima/feebet/feebete.shtml

Cointault, F., P. Sarrazin and M. Paindavoine. 2003. Measurement of the motion of fertilizer particles leaving a centrifugal spreader using a fast imaging system. *Precision Agriculture*, 4, 279-295. Kluwer Academic Publishers, Netherlands.

Fiscus, D. E., G. H. Foster and H. H. Kaufmann. 1969. Grain stream velocity measurements. ASAE Winter Meeting, Dec 9-12, Chicago, Il. Address of ASAE 69-840. 24p.

Kanafojski, C. and T. Karwowski. 1976. *Agricultural machines, theory and construction*. Vol. 2. Foreign Scientific Publications Department of the National Center for Scientific, Technical and Economic Information, Warsaw, Poland.

Karayel, D., M. Wiesehoff, A. Ozmerzi and J. Muller. 2006. Laboratory measurements of seed drill spacing and velocity of fall of seeds using a high speed camera system. *Computers and Electronics in Agriculture*, V50:89-96, Elsevier B.V.

Klenin, N.I., I.F. Popov and V.A. Sakun. 1970. *Agricultural machines: theory of operation*, *computation of controlling parameters and the conditions of operation*. Kolos Publishers, Moscow. 635p.

Lindenburg, F. M. 2004. *Dedicated digital processors*: methods in hardware/software system design. John Wiley & Sons, Ltd., England.

Mason, R. L., R. F. Gunst and J. L. Hess. 2003. *Statistical Design and Analysis of Experiments: with applications to engineering and science*. 2nd edition. John Wiley & Sons, Inc. Hoboken, New Jersey.

Mitchell, B. W. 1983. *Instrumentation and Measurement for Environmental Sciences*. American Society of Agricultural Engineers, St. Joseph, Michigan. p 4-07:4-08.

National Agrability Project. 2003. *Hay Making and Handling Made Easier,* URL: http://www.agrabilityproject.org/assistivetech/tips/hayhandling.cfm.

National Instruments. 2005. CAN bus communication: tutorial. URL: http://www.ni.com/swf/presentation/us/can/

Neale, M. A. 1986. Straw compaction research. *The Agricultural Engineer* 41(4): 126-130.

Neale, M. A. 1989. Research and development for on-farm straw packaging machines. *Agricultural-Progress* 64: 46-57.

New Holland. 1999. BB940 and BB960 Operator's Manual. New Holland North America Inc., New Holland, PA.

Oberg, E., F. D. Jones, H. L. Horton and H. H. Ryffel. 2000. *Machinery Handbook*. 26th Edition. Industrial Press Inc., New York.

Pop, P., P. Eles and Z. Peng. 2004. *Analysis and synthesis of distributed real-time embedded systems*. Kluwer Academic Publishers, Netherlands.

Perry, T. W., A. E. Cullison and R. S. Lowrey. 1999. *Feeds and feeding,* 5th Edition. Prentice Hall., Upper Saddle River, NJ.

Raffel, M., C. Willert and J. Kompenhans. 1998. *Particle Image Velocimetry: A Practical Guide*. Berlin; New York: Springer.

Shinners, K. J., N. G. Barnett and W. M. Schlesser. 2000. Measuring mass-flow rate and moisture on a large square baler. Address of ASAE 001037. 21 pgs.

Sitkei, Gyorgy. 1986. Wafering and pressing of agricultural materials. In *Mechanics of Agricultural Material*. 403-438. Elsevier Science Publishing Co., Inc.

Srivastava, A. K., C. E. Goering and R. P. Rohrbach. 1993. *Engineering principles of agricultural machines*. American Society of Agricultural Engineers, St. Joseph, Michigan. p 383:391.

Stewart, P. 1985, March. Big bales - squeezing more in. *Farm Business* 14-15.

Uziak, J. 1989. Usefulness of different representations of the material in the pressing chamber of a baler to dynamic analysis of a pressing system. Academy of Agriculture, Lublin, Poland. p 2031:2036.

Weisstein, E. W. 1999. Standard Deviation: from Mathworld. Wolfram Research Inc. URL: http://mathworld.wolfram.com/StandardDeviation.html

Yang, Y. and M. D. Schrock. 1993. *Image transformation method for determining kernel motion positions in three dimensions*. Transaction of the ASAE, v 36:1229-1234.

Zurawski, P. E. 2006. *Embedded systems handbook*. Taylor & Francis Group, Boca Raton, FL.

APPENDIX A: SAMPLE CALCULATIONS

1) Pressure Sensor Diaphragm Thickness

2) Calculation of F_{Top} and F_{Bottom} from Scale Readings (North America)

3) Fitting Trend Line to Crop Projectile Plots

4) Conversion of Crank Degrees to Plunger Displacement

5) Calculation of Percent Difference in Weight

1) Pressure Sensor Diaphragm Thickness

Sample calculation for diaphragm thickness of the sensor used on the BB960 in North America (6"). Calculations are based from Oberg et al. 2000 (pg 269).

$$t = \sqrt{\frac{0.39W}{\sigma}} \tag{A.1}$$

where:

W = total applied load (lbs),

σ = maximum tensile stress in plate (lbs/in^2) and

t = thickness of the plate (in).

The maximum tensile stress (σ) for Stainless 316 was approximated to be 205 MPa (29.7x10^3 psi) and the assumed total applied pressure would be 500 kPa (72 psi). With a radius of 76.2 mm (3"), the applied pressure would approximate an applied force of 9.06 kN (2036 lbs). Solving Equation A.1 using the above parameters:

$$t = \sqrt{\frac{0.39(2036)}{29.7 \times 10^3}} = 0.164in = 4.17mm \tag{A.2}$$

2) Calculation of F_{Top} and F_{Bottom} from Scale Readings (North America)

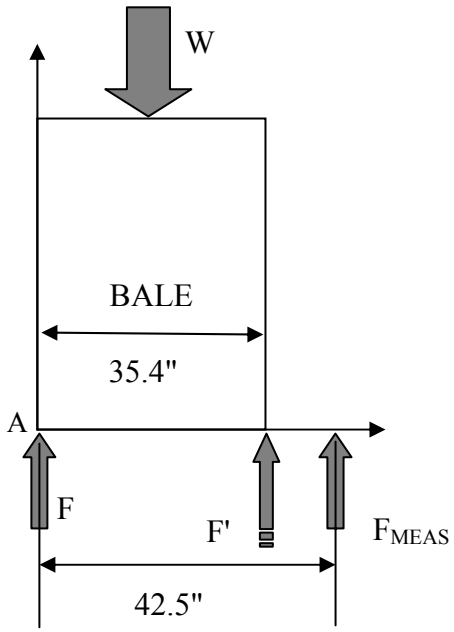

Figure A.1: Calculation of bale weights from scale used in North America

Sample Calculation for bale number 1; F_{MEAS}(Top) = 294, F_{MEAS}(Bottom) = 284 and total measured weight (W) = 695. The measured values were unitless measures from the strain box used. Calculating F'(Top) from F_{MEAS}(Top):

$$F'(Top) = \frac{42.5}{35.4} F_{MEAS}(Top) = \frac{42.5}{35.4}(294) = 353.0 \qquad \text{(A.3)}$$

Using same method, F'(Bottom) = 341.0. Subtracting F' from W, F(Top) = 354.0 and F(Bottom) = 342.0. Averaging F'(Top) and F(Top) together and using a calibration equation to convert into kg; F_{Top} = 159.1 kg and F_{Bottom} = 153.7 kg.

3) Fitting Trend Line to Crop Projectile Plots

Sample calculations for fitting a trend line to Region 1 of side projectile plot.

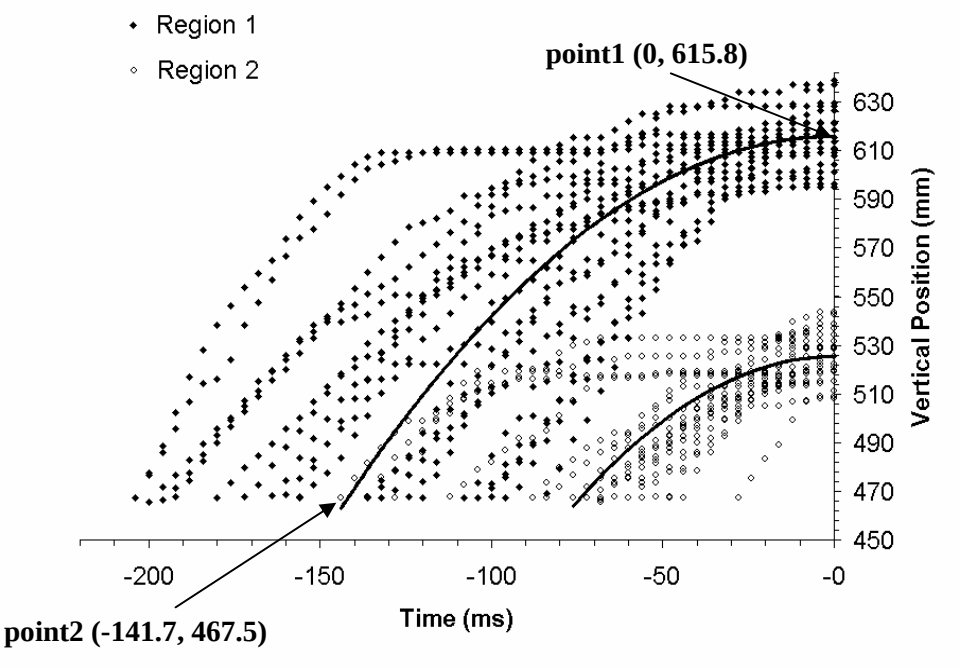

Figure A.2: Calculation of trend line for Region 1

Substituting point1 into Equation 5.3:

$$2a(0) + b = 0 \tag{A.4}$$

Hence,

$$b = 0 \tag{A.5}$$

Substituting point1 into Equation 5.2:

$$615.8 = a(0)^2 + (0)(0) + c \tag{A.6}$$

$$c = 615.8 \tag{A.7}$$

Substituting point2 and resulting coefficients determined in A.5 and A.7 into Equation 5.2:

$$467.5 = a(141.7)^2 + (0)(141.7) + 615.8 \tag{A.8}$$

Solving A.8 for a:

$$a = -0.00738 \tag{A.9}$$

Resulting trend line equation for Region 1:

$$y = -0.00738t^2 + 615.8 \tag{A.10}$$

4) Conversion of Crank Degrees to Plunger Displacement

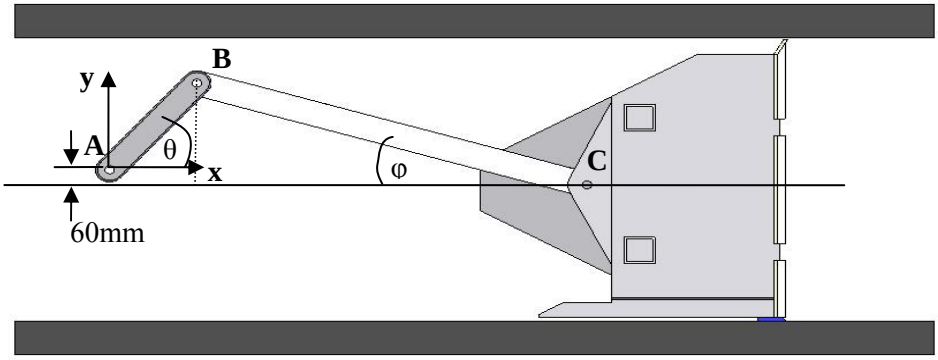

Figure A.3: Geometry of plunger crank assembly

$$\vec{r}_B = \vec{r}_A + \vec{r}_{B/A} \tag{A.11}$$

$$\vec{r}_B = 355\cos(\theta)\hat{i} + 355\sin(\theta)\hat{j} \tag{A.12}$$

And

$$\vec{r}_C = \vec{r}_B + \vec{r}_{C/B} \tag{A.13}$$

$$\vec{r}_C = \vec{r}_B + 1081\cos(\varphi)\hat{i} - 1081\sin(\varphi)\hat{j} \tag{A.14}$$

Where:

$$\varphi = \sin^{-1}\left(\frac{355\sin(\theta) + 60}{1081}\right) \tag{A.15}$$

Therefore

$$\vec{r}_C = 355\cos(\theta)\hat{i} + 355\sin(\theta)\hat{j} + 1081\cos\left[\sin^{-1}\left(\frac{355\sin(\theta)+60}{1081}\right)\right]\hat{i} - 1081\sin\left[\sin^{-1}\left(\frac{355\sin(\theta)+60}{1081}\right)\right]\hat{j} \quad \text{(A.16)}$$

Simplifying

$$\vec{r}_C = 355\cos(\theta)\hat{i} + 1081\cos\left[\sin^{-1}\left(\frac{355\sin(\theta)+60}{1081}\right)\right]\hat{i} - 60\hat{j} \quad \text{(A.17)}$$

Moving coordinate systems from A to C as shown:

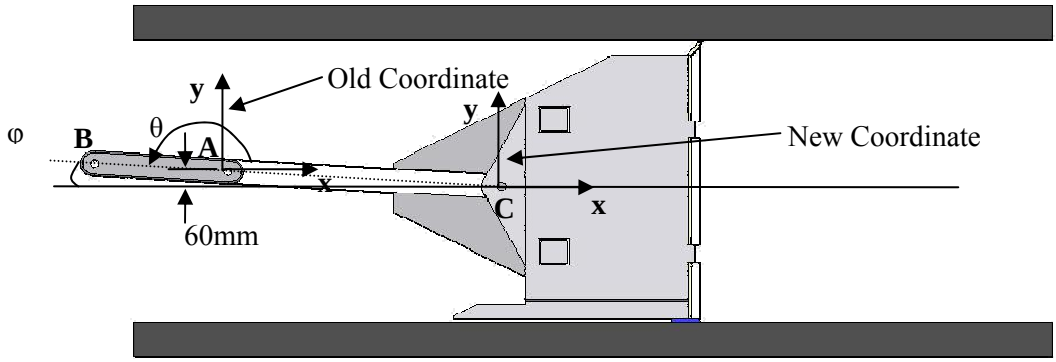

Figure A.4: Geometry of plunger at most forward stroke

Translation of y = -60mm and x:

$$\varphi = \sin^{-1}\left(\frac{60}{1081-355}\right) = 4.74° \quad \text{(A.18)}$$

$$x = (1081 - 355)\cos(4.74°) = 723.5mm \tag{A.19}$$

Hence, plunger position becomes:

$$x_{Position} = 355\cos(\theta + 175.3°) + 1081\cos\left[\sin^{-1}\left(\frac{355\sin(\theta + 175.3°) + 60}{1081}\right)\right] - 723.5 \tag{A.20}$$

where:

θ = Crank position in degrees from most forward plunger position (counter clock wise positive)

5) Calculation of Percent Difference in Weight

$$\%DiffWT = \frac{\left(F_{Top} - F_{Bottom}\right)}{\left(F_{Top} + F_{Bottom}\right)} * 100\% \tag{A.21}$$

where:

%DiffWT = percent difference in weight

For Bale 1, measured F_{Top} = 154 kg and F_{Bottom} = 156 kg. Calculation percent difference in weight:

$$\%DiffWT = \frac{\left(154kg - 156kg\right)}{\left(154kg + 156kg\right)} * 100\% \tag{A.22}$$

$$\%DiffWT = 0.52\% \tag{A.23}$$

APPENDIX B: SUMMARY OF SETTINGS AND MEASURED PARAMETERS

Table B.1: Summary of Settings and Measured Parameters

BALE	Setting			Measured						%DiffWT (%)
	Number	Stuffer	Wall Pressure*	Percent Load (%)	Wall Pressure (MPa)	Stuffer Ratio	Number Flakes	F_{Top} (kg)	F_{Bottom} (kg)	
1	1	4/10	80% CD	81.0	5.77	2.35	23	154	156	0.52
2	1	4/10	80% CD	79.8	5.78	2.67	21	147	150	1.27
3	1	4/10	80% CD	80.9	5.78	1.80	25	160	157	-0.85
4	1	4/10	80% CD	79.9	5.77	2.04	23	157	151	-1.76
5	1	4/10	80% CD	79.9	5.79	2.13	23	142	142	0.00
6	1	4/10	80% CD	81.2	5.69	2.39	23	141	151	3.51
7	1	4/10	80% CD	81.3	5.70	2.20	25	167	168	0.32
8	1	4/10	80% CD	81.4	5.71	2.56	25	164	163	-0.33
9	1	4/10	80% CD	81.6	5.72	2.04	24	178	173	-1.54
10	3	4/10	11 MPa	93.2	11.04	1.50	48	185	198	3.39
11	2	1/10	11 MPa	82.6	11.03	1.00	81	179	173	-1.56
12	4	8/10	11 MPa	85.8	10.85	2.50	32	176	190	3.84
13	2	1/10	11 MPa	83.8	11.07	1.00	68	186	186	0.13
14	3	4/10	11 MPa	84.3	11.09	1.66	44	171	190	5.13
15	4	8/10	11 MPa	81.2	10.99	2.00	34	172	192	5.64
16	3	4/10	11 MPa	80.8	10.92	1.93	41	179	191	3.25
17	2	1/10	11 MPa	72.4	10.82	1.10	70	188	172	-4.44
18	4	8/10	11 MPa	83.6	11.01	2.40	35	177	178	0.42
19	7	8/10	7 MPa	50.1	6.94	2.21	28	143	152	3.06
20	5	1/10	7 MPa	45.3	6.96	1.24	59	162	162	0.00
21	6	4/10	7 MPa	48.4	6.93	2.26	35	135	132	-0.94
22	7	8/10	7 MPa	43.7	6.83	2.15	27	135	146	3.74
23	5	1/10	7 MPa	42.3	6.82	1.02	54	147	153	2.00
24	6	4/10	7 MPa	44.0	6.76	1.66	38	148	162	4.68
25	6	4/10	7 MPa	44.6	6.92	1.77	35	150	154	1.32
26	5	1/10	7 MPa	47.8	7.02	1.06	54	165	146	-6.11
27	7	8/10	7 MPa	46.8	6.95	2.68	28	139	150	3.82
28	4	8/10	11 MPa	89.5	10.93	2.00	32	193	206	3.27
29	3	4/10	11 MPa	75.6	10.94	1.52	44	172	192	5.36

*CD = constant density

APPENDIX C: SAS SAMPLE CODE AND RESULTS

Refer to Appendix E for a complete listing of SAS inputs and outputs.

C.1 - Comparison of Means - Input

The following is a sample SAS code for comparison of top and bottom plunger pressures or each setting.

```
data Top_vs_Bot_Duncan;
input bale rep setting region$ press;
cards;

1   1     1     TL    560.0761105
1   2     1     TL    380.1322156
1   3     1     TL    359.7123045
1   4     1     TL    510.0719381
1   5     1     TL    576.7584727
1   6     1     TL    665.5884098
1   7     1     TL    493.2107969
1   8     1     TL    466.5359627
↓
29  41    3     BC    259.9232467
29  42    3     BC    312.3852261
29  43    3     BC    326.9391284
29  44    3     BC    277.0579781
;

proc sort;
by setting;
run;

proc glm;

class bale setting region;
model press = bale setting region;
means region/Duncan;
by setting;

means region;
by setting;

run;
```

C.2 - Comparison of Means – Output present it as table with borders

The following is a sample output for setting 1. For complete results refer to Appendix E.

---------- setting=1 ----------

The GLM Procedure

Class Level Information

Class	Levels	Values								
bale	9	1	2	3	4	5	6	7	8	9
setting	1	1								
region	4	BC	BL	TC	TL					

Number of observations 848

Dependent Variable: Press

Source	DF	Sum of Squares	Mean Square	F Value	Pr > F
Model	11	24852852	2259350.15	125.17	<.0001
Error	836	15089879	18050.09		
Corrected Total	847	39942731			

R-Square	Coeff Var	Root MSE	press Mean
0.622212	44.18786	134.3506	304.0442

Source	DF	Sum of Squares	Mean Square	F Value	Pr > F
bale	8	441734.4	55216.8	3.06	0.0021
setting	0	0	.	.	.
region	3	24411117	8137039.08	450.8	<.0001

Source	DF	Sum of Squares	Mean Square	F Value	Pr > F
bale	8	441734.4	55216.8	3.06	0.0021
setting	0	0	.	.	.
region	3	24411117	8137039.08	450.8	<.0001

Duncan's Multiple Range Test for press

NOTE: This test controls the Type I comparisonwise error rate, not the experimentwise error rate.

Alpha	0.05
Error Degrees of Freedom	836
Error Mean Square	18050.09

Number of Means	2	3	4
Critical Range	25.61	26.97	27.87

Means with the same letter are not significantly different.

Duncan Grouping	Mean	N	region
A	494.02	212	TL
B	403.42	212	BL
C	276.23	212	BC
D	42.5	212	TC

Level of region	N	----------press----------	
		Mean	Std Dev
BC	212	276.235	68.253658
BL	212	403.42	70.994894
TC	212	42.49893	229.54328
TL	212	494.023	105.92728

…

C.2 – Regression Model - Input

The following is the sample SAS code for development of the regression model. For complete code refer to Appendix E.

```
data stepwise_RegII;
input bale DiffPress ChamPress PLoad … StuffRNumFlake FlakeSetNumFlake DiffWT;
cards;

1   87.99822456   5.771423989   80.98812658   …   54   92   -1.621
↓
27  17.61997766   6.954634611   46.76874121   …   75   224  11
;


proc reg;

model DiffWT = DiffPress ChamPress PLoad StuffR FlakeSet NumFlake
DiffPressChamPress DiffPressPLoad DiffPressStuffR DiffPressFlakeSet
DiffPressNumFlake ChamPressPLoad ChamPressStuffR ChamPressFlakeSet
ChamPressNumFlake PLoadStuffR PLoadFlakeSet PLoadNumFlake StuffRFlakeSet
StuffRNumFlake FlakeSetNumFlake / selection=MAXR;

run;
```

C.2 – Regression Model - Output

The following is the SAS output for stepwise regression up to the best one variable regression model. For complete output, refer to Appendix E.

The REG Procedure
Model: MODEL1
Dependent Variable: DiffWT

Maximum R-Square Improvement: Step 1

Variable FlakeSetNumFlake Entered: R-Square = 0.4710 and C(p) = .

Analysis of Variance

Source	DF	Sum of Squares	Mean Square	F Value	Pr > F
Model	1	942.4565	942.4565	16.03	0.0008
Error	18	1058.54	58.80779		
Corrected	Total	19	2000.997		

Parameter Standard

Variable	Estimate	Error	Type II SS	F Value	Pr > F
Intercept	-9.88794	3.80053	398.0689	6.77	0.018
FlakeSetNumFlake	0.09488	0.0237	942.4565	16.03	0.0008

Bounds on condition number: 1, 1

The above model is the best 1-variable model found.

APPENDIX D: RESULTS

1) Tabular Strain Results for Side View

2) Mean Comparisons Between Peak Plunger Pressure Repetitions

3) Plunger Pressure Profiles for Each Setting

1) Crop Strain Results for Side View

Table D.1: Strain Results - Side View

	AVERAGE		PEAK	
	Top	Bottom	Top	Bottom
Flake 1	0.300	0.050	0.439	0.162
Flake 2	0.232	0.190	0.417	0.385
Flake 3	0.035	0.117	0.172	0.184
Flake 4	0.273	0.160	0.465	0.272
Flake 5	0.167	0.076	0.259	0.122
Flake 6	0.202	-0.009	0.266	0.012
Flake 7	-0.194	0.107	0.021	0.196
Flake 8	0.252	-0.003	0.382	0.073
Flake 9	0.083	0.092	0.157	0.188
Flake 10	-0.015	0.164	0.067	0.265
Flake 11	0.168	0.019	0.365	0.095
Flake 12	0.001	0.092	0.028	0.135
Flake 13	0.237	-0.017	0.376	0.100
Flake 14	0.137	0.154	0.217	0.280
Flake 15	-0.005	-0.162	0.087	-0.235
Flake 16	0.233	-0.176	0.318	-0.300
Flake 17	0.384	-0.266	0.493	0.063
Flake 18	0.226	0.050	0.265	0.096
Flake 19	0.072	-0.003	0.151	0.027
Flake 20	-0.080	-0.151	-0.219	-0.240
Flake 21	0.138	0.017	0.239	0.061
Flake 22	0.263	-0.028	0.450	0.053
Flake 23	-0.043	-0.166	-0.085	-0.243
Flake 24	0.123	0.193	0.262	0.349
Flake 25	0.006	0.024	0.061	0.067
Average	0.128	0.021	0.226	0.087
StDev	0.139	0.125	0.183	0.181

2) Comparison Between Peak Plunger Pressure Repetitions

Table D.2: Comparison of Peak Plunger Pressures for Setting 1

Setting	Region	Bale Number	Mean (kPa)	Std Dev (kPa)	Duncan Grouping	Number of Flakes
1	TL	9	562	101	A	24
		1	542	90	B A	23
		3	537	98	B A	25
		2	511	99	B A C	21
		8	503	108	B A C	25
		7	484	87	B D C	25
		5	455	105	E D C	23
		6	440	74	E D	23
		4	406	96	E	23
	BL	1	464	70	A	23
		8	408	66	B	25
		6	408	70	B	23
		7	406	85	B	25
		5	402	77	B	23
		3	395	63	B	25
		2	388	71	B	21
		9	382	48	B	24
		4	377	55	B	23
	TC	2	192	116	A	21
		3	100	222	B A	25
		8	90	188	B A	25
		5	78	200	B A	23
		4	68	195	B A	23
		7	62	219	B A	25
		9	36	235	B	24
		6	-7	245	B	23
		1	-234	201	C	23
	BC	6	305	67	A	23
		7	300	93	B A	25
		2	287	63	B A C	21
		4	284	53	B A C	23
		5	272	62	B A C	23
		1	268	86	B A C	23
		3	263	53	B A C	25
		9	260	58	B C	24
		8	250	56	C	25

Table D.3: Comparison of Peak Plunger Pressures for Settings 2-7

Settimng	Region	Bale Number	Mean (kPa)	Std Dev (kPa)	Duncan Grouping	Number of Flakes
2	TC	17	323	50	A	70
		13	306	50	B	68
		11	275	46	C	81
	BC	11	285	32	A	81
		13	281	44	A	68
		17	280	34	A	70
3	TC	10	466	86	A	48
		29	358	73	B	44
		16	327	52	C	41
		14	313	52	C	44
	BC	10	414	82	A	48
		16	301	37	B	41
		29	300	43	B	44
		14	262	34	C	44
4	TC	28	382	57	A	32
		18	314	79	B	35
		12	294	76	B	32
		15	283	53	B	34
	BC	12	365	41	A	32
		28	338	50	B	32
		15	288	48	C	34
		18	286	47	C	35
5	TC	20	247	52	A	59
		26	241	49	A	54
		23	232	47	A	54
	BC	20	221	34	A	59
		23	219	33	A	54
		26	211	31	A	54
6	TC	21	239	45	A	35
		24	236	46	A	38
		25	232	41	A	35
	BC	21	206	33	A	35
		25	183	25	B	35
		24	170	25	C	38
7	TC	27	225	50	A	28
		19	219	58	A	28
		22	211	41	A	27
	BC	19	191	26	A	28
		27	188	26	A	28
		22	186	31	A	27

3) Pressure Profiles for Each Setting

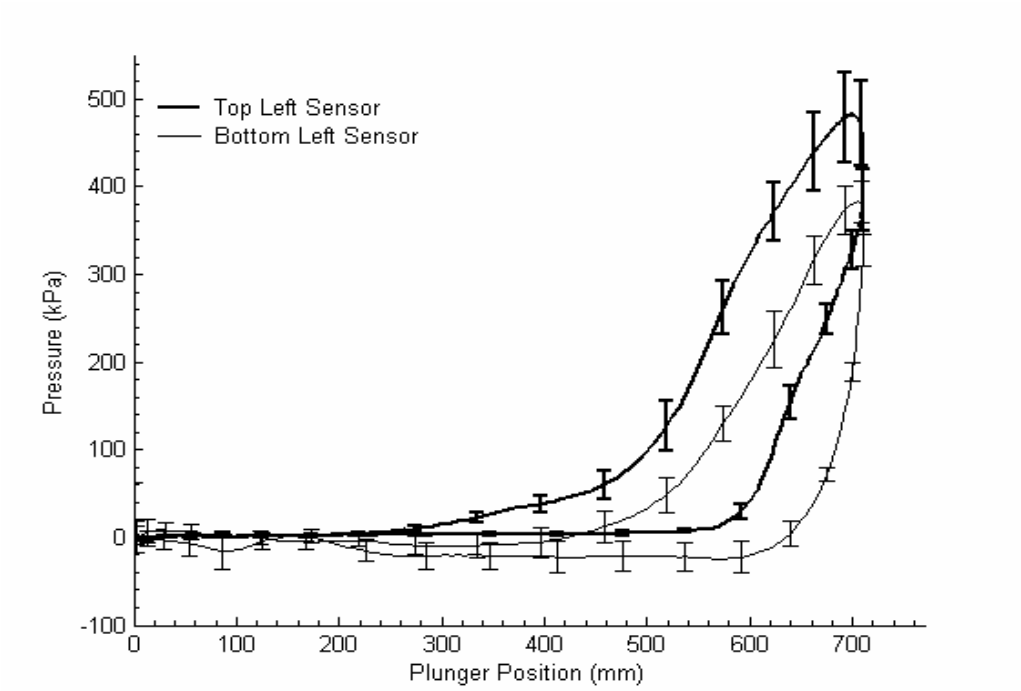

Figure D.1: Pressure profiles for Setting 1 (Left Sensors)

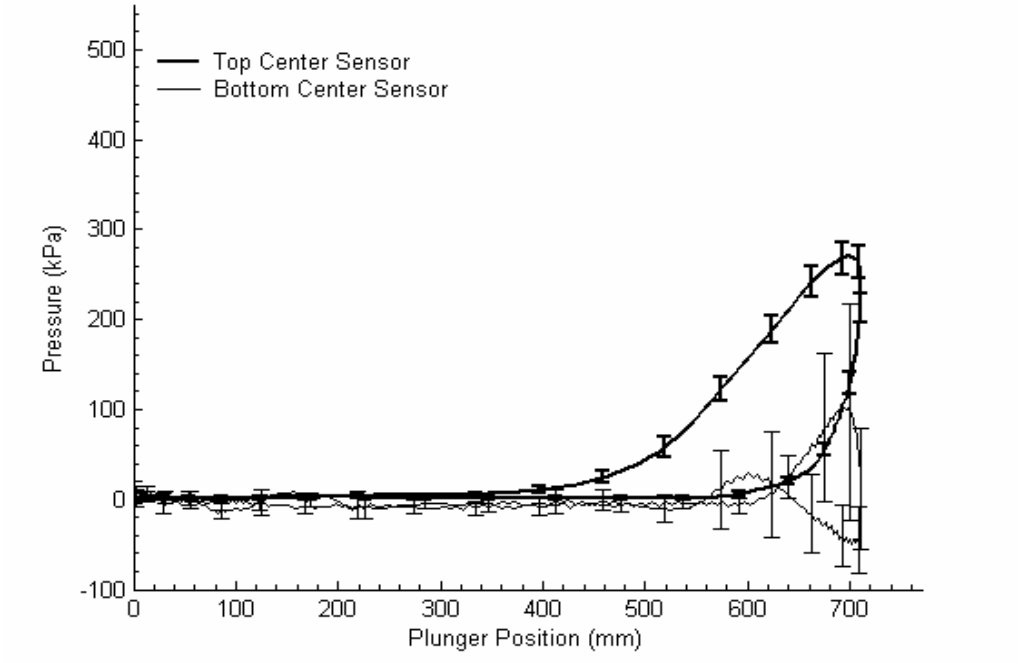

Figure D.2: Pressure profiles for Setting 1 (Center Sensors)

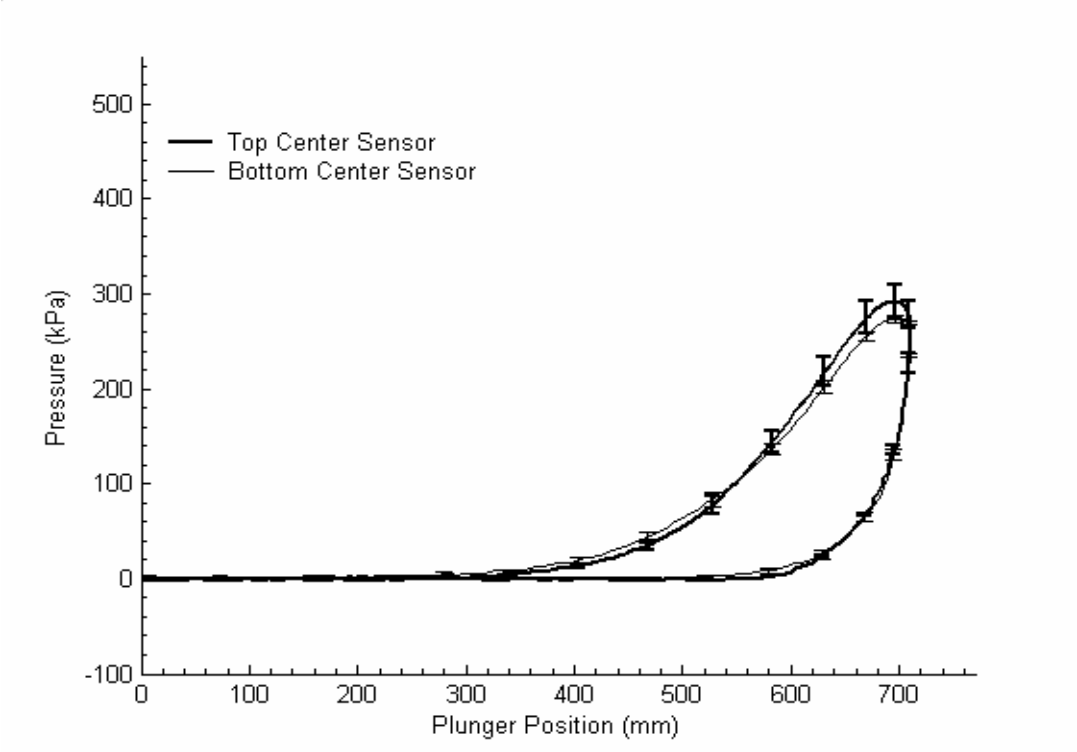

Figure D.3: Pressure profiles for Setting 2

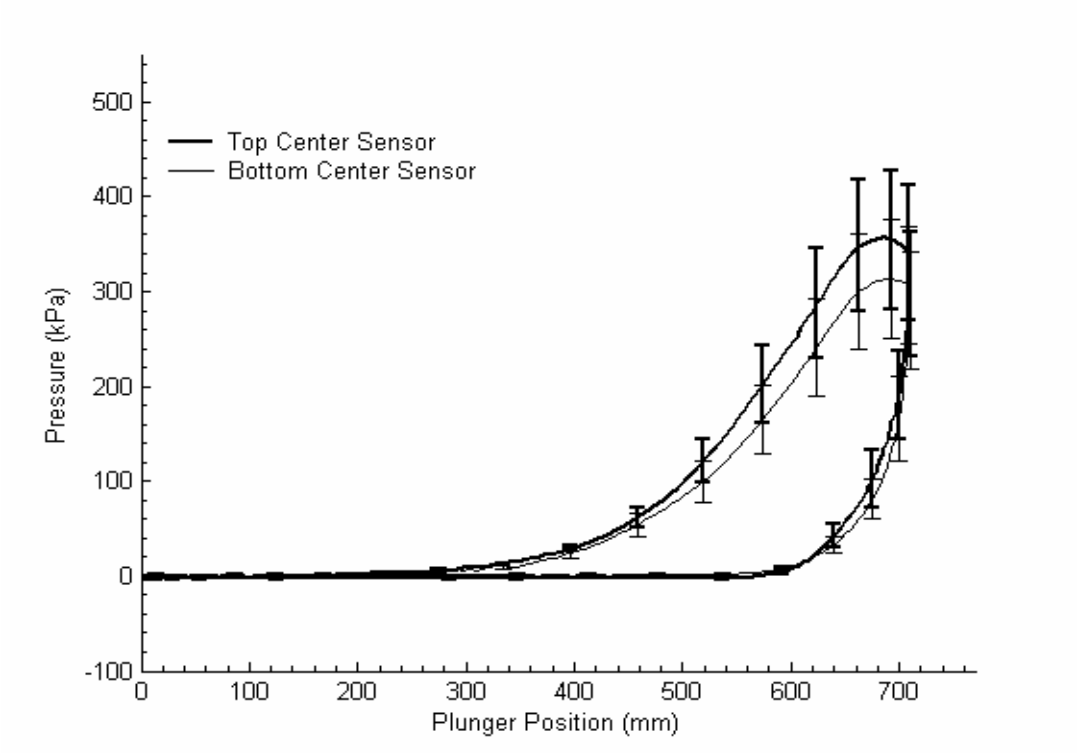

Figure D.4: Pressure profiles for Setting 3

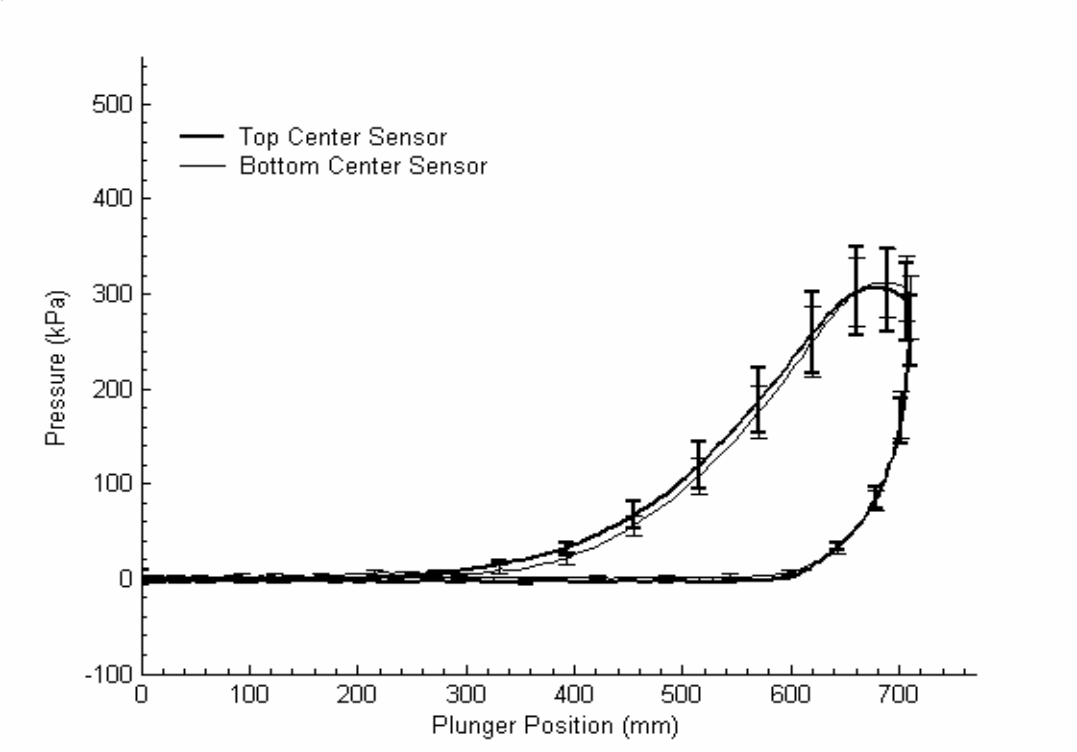

Figure D.5: Pressure profiles for Setting 4

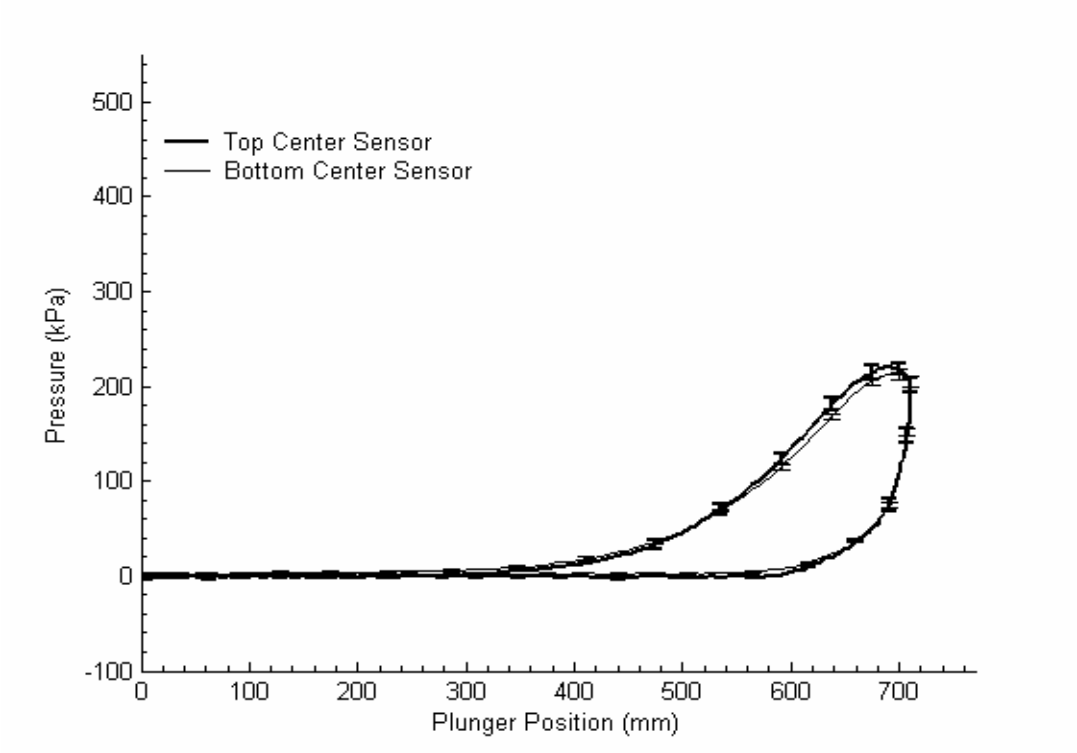

Figure D.6: Pressure profile for Setting 5

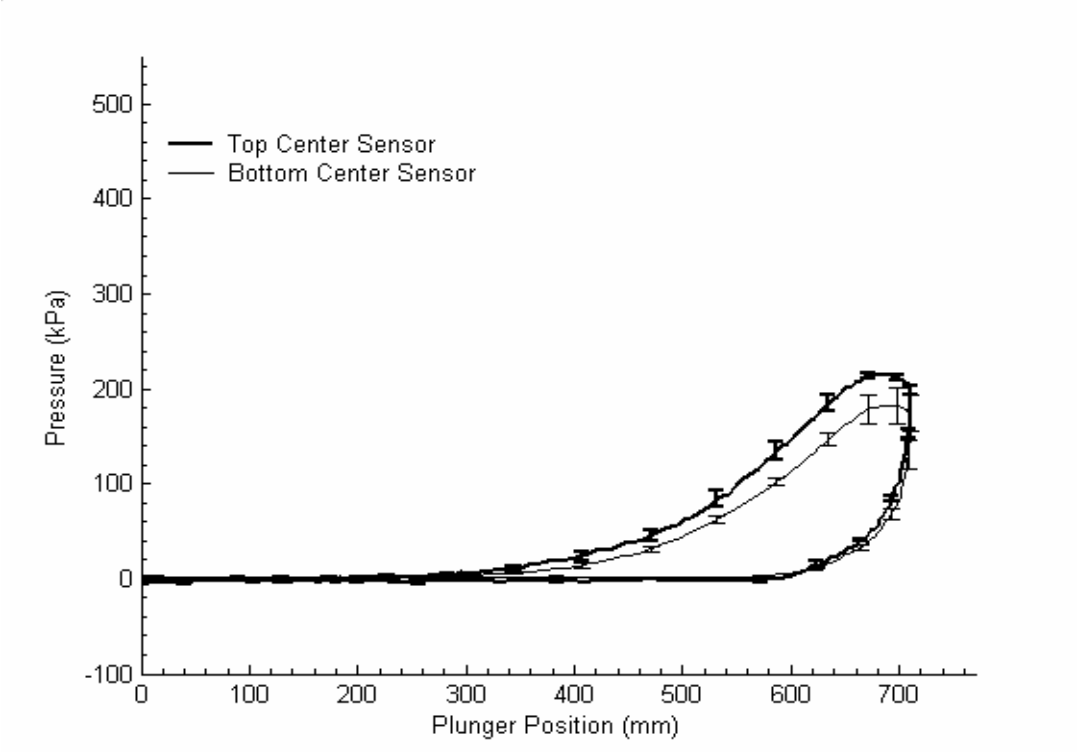

Figure D.7: Pressure profile for Setting 6

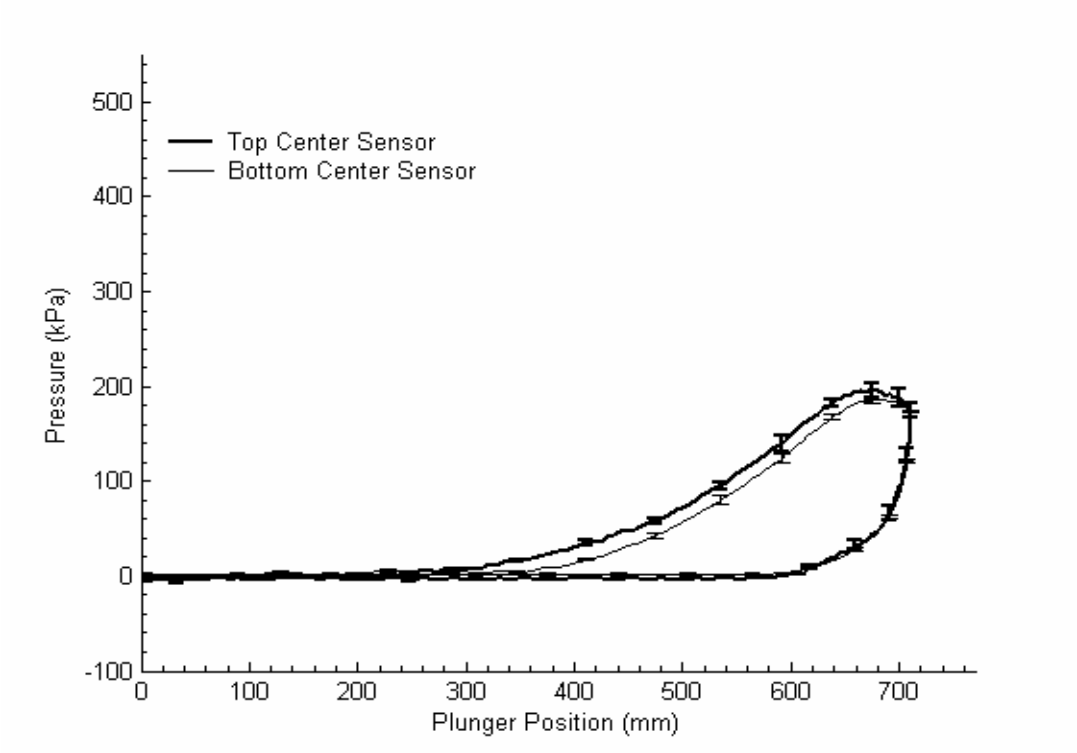

Figure D.8: Pressure profile for Setting 7

APPENDIX E: ELECTRONIC FILES

The electronic files discussed throughout this thesis are included on the accompanying CD. Figure E.1 illustrates the central folders on the accompanying CD.

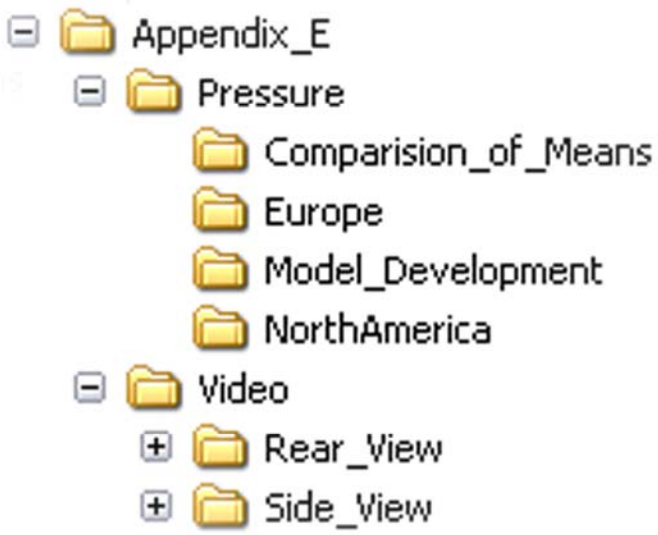

Figure E.1: List of Electronic Files on the Accompanying CD

The electronic files been divided into two main folders ("Pressure" and "Video") to distinguish between the pressure and video analysis. For the pressure files, the folders entitled "Europe" and "NorthAmerica" contain sample analysis code for MS Excel VBA and raw pressure data. The folders entitled "Comparison_of_Means" and "Model_Development" contain sample SAS code and output. The "Video" folder contains information regarding both side and rear video analysis. Both folders contain sample high speed video of the crop's trajectory, AutoCAD™ analysis file with Visual Basic™ Module and a folder containing sample extracted images of a video recording.

Directions on accessing and operating the analyses files are provided in the "Read_Me" text file located in the root directory "Appendix_E". Descriptions of the Microsoft Excel macros used for the pressure analysis are listed in Tables E.1 – E.3.

Table E.1: MS Excel Macros Used for Analysis of NA CAN Data

Call	Step #	Macro Name	Description and Notes
	1	NA	Import correct: identifier, code(x8), Time(hr, min, sec & ms)
A	2	FormatSheetCAN	Inserts Rows, Column Labels, Color identifier
A	3	TimeCAN	Takes date stamp from file and converts to time of run
A	4	CANID	Takes Hex Value and converts to 11-bit ID
A	5	CodeCAN	Determine values of: Load, Bale Chamber, Stuffer and Knotter
A	6	DataNumCAN	Creates equivalent DAQ # for run (250 samples/ second)
B	7	ModeError	Removes any signals occurring at the same time
B	8	DAQ_Number	Creates in DAQ scale of numbers
B	9	DAQ_Timed	Times CAN signals with DAQ scale of numbers
B	10	ZeroAndOnlyZero	Finds center of knotter signal for analysis
B	11	Stuffer4Count	Counts stuffer strokes in the bale
D	INT STEP	AlignCANCopy	Highlights alignment pt, outputs # for alignment, copies data

Table E.2: MS Excel Macros Used for Analysis of NA DAQ Data

Call	Step #	Macro Name	Description and Notes
C	1	deleteExcessCells	Removes invalid data pts (-5) resulting from ending of run
C	2	TopHeader	Formats top of LVM file
C	3	StufferDiv	Divides DAQ stuffer by set value (default 3)
C	4	DigTDC	Converts analog plunger DAQ signal into dig 1's & 0's
C	5	OneAndOnlyOne	Determines TDC from Dig TDC - only 1 value for TDC
C	6	AlignDAQ	Finds point on DAQ data file where CAN should be aligned and highlights it. Warning: Do not move cell location
	INT STEP	(NA)	GOTO CAN FILE AND RUN INT STEP
E	7	CANDAQPaste	Pastes the copied data to correct location. Keep in same cell location from previous step!!
E	8	VerifyPlot	used to verify the CAN data was aligned correctly *Things to look for: -comparison btwn DAQ & CAN stuffer -Complete Knotter Cycle -Pressure rise & drop @ correct time **DELETE Plot when finished

F	9	CopyBounds	Creates new sheet called ___ Bounds and copies all data to new sheet
F	10	BoundsFormat	Inserts headers for bounds & new data #'s
G	11	MovingAverageCh1	Removes noise from channel 1 using a moving average
H	12	MovingAverageCh3	Removes noise from channel 3 using a moving average
I	13	StufferAndTDC	Finds where both stuffer has engaged and TDC (for Triggering)
I	14	MaxCount	Determines maximum plunger stroke count using StufferAndTDC Output - Cell "AA3"
I	14a	VerifyPlot2	Macro to view TDC/Stuffer w/ Bounds ***DELETE Plot when finished
J	15	SettingAnalysis	Finds avg, std dev, variance, max & min of BaleChamber & Load for copy to analysis sheet
J	16	StrokeCount	Creates new sheet entitled Analysis & copies relavent data to new sheet statistical Analysis for: -stroke count -Bale Chamber Pressure -% Load -Stuffer Ratio
K	17	ZeroAmp	Zero's every plunger stroke to account for drift
L	18	CopyChannels	Creates 5 new Sheets (Channel 0 -3 & AllChannels) Inserts plunger displacement in each sheet Inserts pressure of each stroke into individual columns centered at BDC
L	19	FormatChannels	-Avg each channel -Inserts Pressure Equation -Copy Avg Pressure & Pastes in AllChannels Sheet -Formats Headers of each Sheet -Finds Maximum Pressure
M	20	SAS_Ready	Copies data into new sheet. Data is in format for use in SAS

Table E.3: MS Excel Macros Used for Analysis of EU Pressure Data

Call	Step #	Macro Name	Description and Notes
A	1	EUDigTDC	Converts analog plunger DAQ signal into dig 1's & 0's
A	2	EUOneAndOnlyOne	Determines TDC from Dig TDC - only 1 value for TDC
B	3	EUshiftCAN	Shifts CAN data down one plunger stroke
C	4	EUZeroAndOnlyZero	Finds center of knotter cycle
C	5	EUStuffer4Count	Finds stuffer reset
D	6	EUCopyBounds	Creates new sheet called ___ Bounds and copies all data to new sheet
D	7	EUBoundsFormat	Inserts headers for bounds & new data #'s
E	8	EUStufferAndTDC	Finds where both stuffer has engaged and TDC (for Triggering)
E	9	EUMaxCount	Determines maximum plunger stroke count using StufferAndTDC
F	10	EUSettingAnalysis	Finds avg, std dev, variance, max & min of BaleChamber & Load for copy to analysis sheet
F	11	EUStrokeCount	Creates new sheet entitled Analysis & copies relavent data to new sheet statistical Analysis for: -stroke count -Bale Chamber Pressure -% Load -Stuffer Ratio
G	12	EUCopyChannels	Creates 5 new Sheets (Channel 0 -3 & AllChannels) Inserts approximate plunger displacement in each sheet Inserts pressure of each stroke into individual columns centered at BDC
G	13	EUFormatChannels	-Avg each channel -Inserts Pressure Equation -Copy Avg Pressure & Pastes in AllChannels Sheet -Formats Headers of each Sheet -Finds Maximum Pressure
H	14	EU_SAS_Ready	
I	15	Transfer_BB960	Transfers data to new book called "BB960_Results.xls"